Master's Thesis
석사 학위논문

Study of Noise-Induced Tracking Error Phenomenon in Systems with Anti-windups

Juseung Lee(이 주 승 李 柱 昇)

Department of Information and Communication Engineering
정보통신융합공학전공

DGIST

2015

Master's Thesis
석사 학위논문

Study of Noise-Induced Tracking Error Phenomenon in Systems with Anti-windups

Juseung Lee(이 주 승 李 柱 昇)

Department of Information and Communication Engineering
정보통신융합공학전공

DGIST

2015

Study of Noise-Induced Tracking Error Phenomenon in Systems with Anti-windups

Advisor : Professor Yongsoon Eun

Co-advisor : Professor Jonghyun Kim

by

Juseung Lee

Department of Information and Communication Engineering

DGIST

A thesis submitted to the faculty of DGIST in partial fulfillment of the requirements for the degree of Master of Science in the Department of Information and Communication Engineering. The study was conducted in accordance with Code of Research Ethics[1]

05(month). 19(day). 2015(year)

Approved by

Professor 은 용 순 (Signature)
(Advisor)

Professor 김 종 현 (Signature)
(Co-Advisor)

[1] Declaration of Ethical Conduct in Research: I, as a graduate student of DGIST, hereby declare that I have not committed any acts that may damage the credibility of my research. These include, but are not limited to: falsification, thesis written by someone else, distortion of research findings or plagiarism. I affirm that my thesis contains honest conclusions based on my own careful research under the guidance of my thesis advisor.

Study of Noise-Induced Tracking Error Phenomenon in Systems with Anti-windups

Juseung Lee

Accepted in partial fulfillment of the requirements for the degree of Master of Science.

05(month). 19(day). 2015(year)

Head of Committee ________________(인)

Prof. Yongsoon Eun

Committee Member_________________(인)

Prof. Jonghyun Kim

Committee Member________________(인)

Prof. Kyung-Joon Park

MS/IC
201324010

이 주 승. Juseung Lee. Study of Noise-Induced Tracking Error Phenomenon in systems with Anti-windups. Department of Information and Communication Engineering. 2015. 60p. Prof. Eun, Yongsoon. Co-Advisors Prof. Kim, Jonghyun.

ABSTRACT

PI controller has been widely used in various industrial fields and played important role of eliminating the tracking error. In PI controlled system with saturation actuator, method called “Anti-windup” has been used for avoiding undesirable phenomenon such as performance degradation, instability, and windup [2-3]. In PI controlled systems with anti-windup, tracking loss due to measurement noise has been recently discovered, where measurement noise persistently triggers anti-windup mechanism in a certain operation range that result in non-zero steady state tracking error, which was called “Noise Induced Tracking Error (NITE)” [10]. Such a system was analyzed under both zero-mean Gaussian noise and quantification of the tracking loss is given in terms of system parameters and noise standard deviation.

In this work, we show that NITE could occur in all PI controlled systems if both anti-windup and measurement noise exist, regardless of anti-windups. We also extend the existing results to a case with uniformly distributed noise. Using stochastic averaging approach, we quantify the noise induced tracking error with respect to system parameters and noise characteristics, and shows that the phenomenon of tracking loss occurs with uniformly distributed noise as well. Conditions under which the tracking loss occurs are derived. The result is compared with that under zero mean Gaussian noise with the same level of standard deviation.

We suggest two solutions to prevent NITE. One method is using a virtual saturation. We explain how effective the virtual saturation to mitigate NITE. An analysis of internal stability based on linear matrix inequalities is conducted on the system with a virtual saturation. The other method is changing static P gain to dynamic P gain. Dynamic P gain plays the role of eliminating an effect of noise in the systems. The result shows that NITE does not occur due to the two solutions. We also show the differences between two solutions.

Keywords: Noise induced tracking error, Saturating actuator, PI control, Anti-windup, Measurement noise

Contents

List of Figures

List of Figures

Ⅰ. INTRODUCTION

1.1 Motivation

In linear systems, proportional-integral (PI) controller is used in various industrial applications and one of necessary methods for eliminating tracking error. It is however, required to consider nonlinear effects because saturation actuator is present in most of all systems [1]. In the case of PI controlled systems with saturation actuator, the phenomenon called *Windup* occurs due to controller with integral action and have adverse effects such as instability, and performance degradation on the systems [2-3].
In order to mitigate the phenomenon of windup, Anti-windup strategies can be used in the systems [4-6]. Various anti-windup strategies has been researched and used widely in industrial fields [7-10].
Recently, In PI controlled systems with anti-windup called *back-calculation* [11], tracking loss due to measurement noise has been discovered, where measurement noise persistently triggers anti-windup mechanism in a certain operation range that result in non-zero steady state tracking error. This non-zero steady state tracking error was named Noise-Induced Tracking Error (NITE) [10].
In this work, we shows that NITE could occur in all systems with integral controller if both anti-windup and measurement noise exist, regardless of anti-windups. This fact means that NITE is one of new problems and important issue in many different fields, where control system can be used.

1.2 Purpose

In this paper, we show that NITE occurs in PI controlled systems with anti-windup structures shown in [12-13] and then the quantification of the tracking error is given in terms of system parameters and noise standard deviation by using stochastic averaging theory introduced in [14]. Such a system is analyzed under both zero-mean Gaussian noise and uniformly distributed noise and NITE caused by Gaussian noise is compared with that caused by uniformly distributed noise.
In order to mitigate NITE, some solutions are required. We suggest two solutions to avoid the phenomenon of NITE. One solution is a virtual saturation, which has a larger value of saturation bound than that of actual saturation actuator bound. By using stochastic averaging theory, we quantify NITE in terms of PI controlled systems with the virtual saturation and compare it with PI controlled systems without the virtual saturation.

In addition, we suggest a method determining a stability of the systems with a virtual saturation based on Linear Matrix Inequalities (LMI). The other solution is transforming static proportional gain into dynamic proportional gain of controller. Both of two solutions is useful methods to prevent NITE. We compare these two solutions and show some characteristics of each of them by using MATLAB simulation.

1.3 Outline

The outline of this paper is as follows: the problem statement is given in Chapter Ⅱ. The analysis for the systems is carried out using stochastic averaging theory and the result of a case with uniformly distributed noise is compared with that of a case with Gaussian noise in Chapter Ⅲ. Key solutions to Noise Induced Tracking Error are provided in Chapter Ⅳ. In chapter Ⅴ, we show that NITE occurs by using a specific system. Conclusion is given in Chapter Ⅵ.

Ⅱ. Problem statement

2.1 Anti-windups

Figure 1 shows the PI controlled systems subject to actuator saturation. *P(s)* is the plant, K_p and K_i are proportional gain, and integral gain. The signals *r, e, y, n, d, u* are, respectively, reference, tracking error, output, measurement noise, disturbance, and control input. $\mathrm{sat}_{\alpha}^{\beta}(u)$ is saturation actuator, which is in the first position of the system to be controlled commonly in most previous researches [4][15-17] and defined by

$$\mathrm{sat}_{\alpha}^{\beta}(u)=\begin{cases}\alpha, & u<\alpha\\ \beta, & u>\beta\\ u, & \alpha\le u\le\beta\end{cases} \tag{1}$$

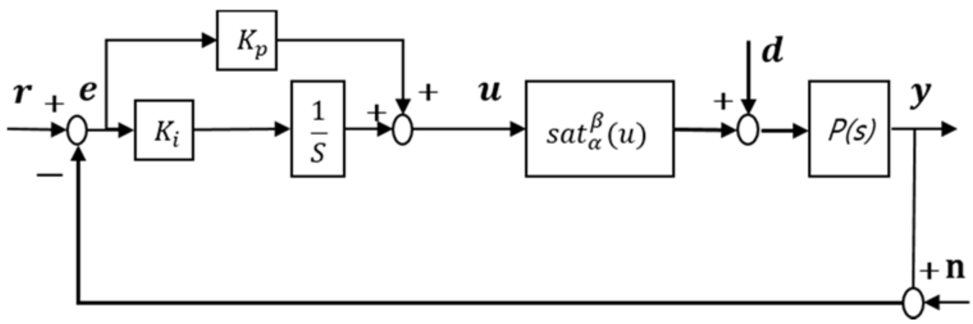

Figure 1. PI controlled systems with saturation actuator

There are various anti-windup strategies in order to avoid adverse effects due to actuator saturation. We show anti-windup structures applicable to PI controlled systems in Figures 2(a), (b), (c) and (d). Anti-windup structures of Figure2 (a), (b), and (c) are, respectively, called back-calculation, dynamic full authority, and dynamic external global. K_{AW} is anti-windup gain, which is marked as $K_{AW,1}$and

$K_{AW,2}$ in order to distinguish between themselves. $K_{AW,1}(s)$ and $K_{AW,2}(s)$ mean dynamic blocks of anti-windup gains. Figure 2 (a) shows the anti-windup gain affect to the control system by injecting their output signals into the state of integral controller. Figure 2 (b) shows the anti-windup blocks affect to the control system by injecting their output signals into both the controller output and the state of integral controller. Figure 2 (c) also, shows that the control system is affected by anti-windup blocks only at the input and output.

Anti-windup structure of Figure 2 (d) is introduced in [13] and the system of Figure 2 (d) is equivalent to PI controlled system. Unlike anti-windup structures of Figures 2 (a), (b) and (c), the system of Figure 2 (d) involves anti-windup without specific anti-windup gain such as K_{AW}.

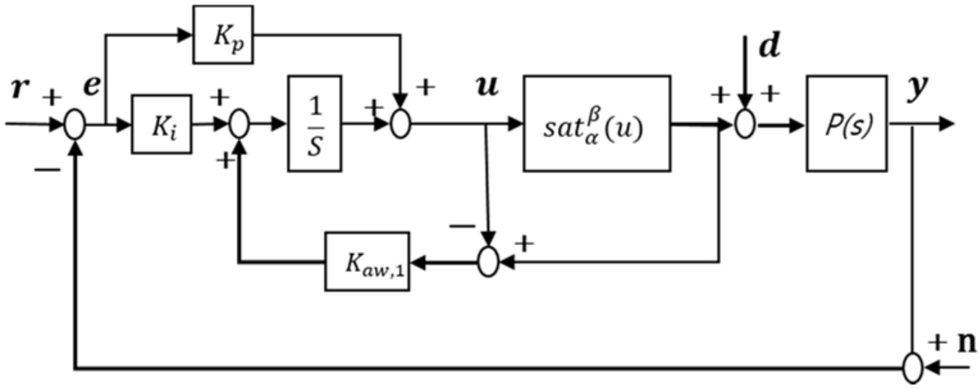

Figure 2 (a). PI system with back-calculation anti-windup

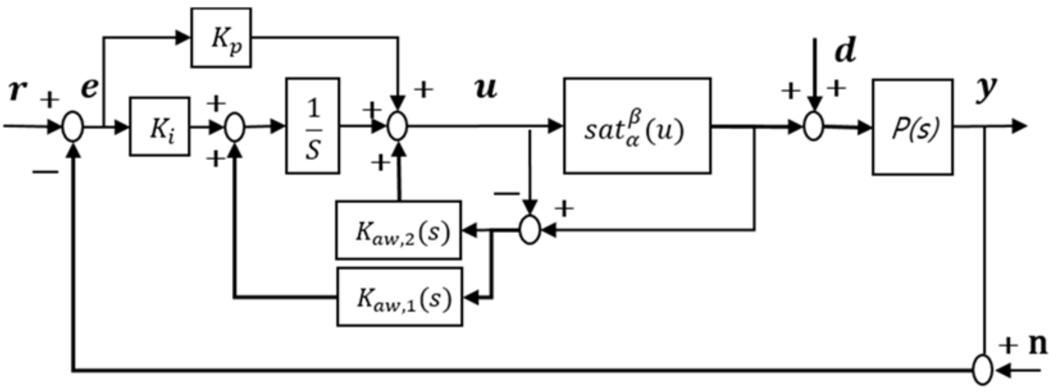

Figure 2 (b). PI system with dynamic full authority anti-windup

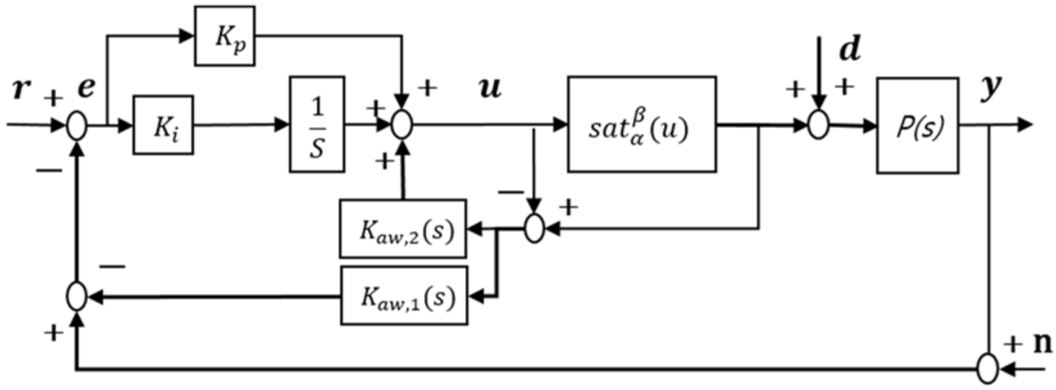

Figure 2 (c). PI system with dynamic external global anti-windup

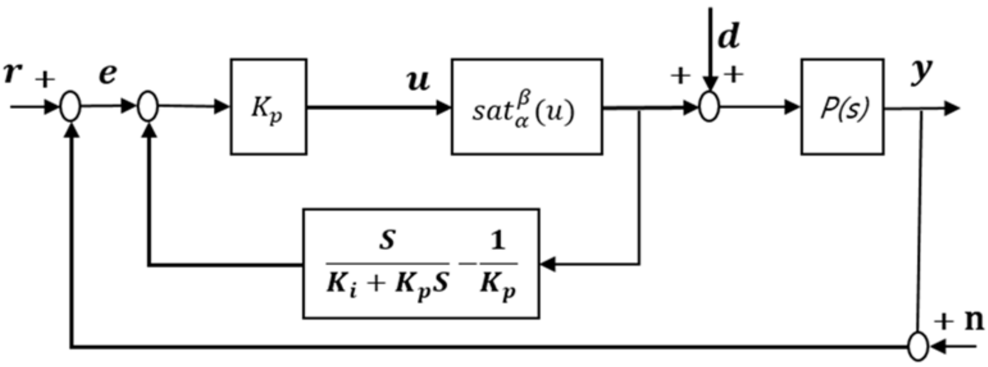

Figure 2 (d). PI system with anti-windup referred to [13]

In Chapter Ⅲ, we show that NITE could occur in all PI controlled systems with anti-windup structures through the Figures 2 (a), (b), (c), and (d) and quantify NITE in terms of the characteristic of both the system parameters and measurement noise.

2.2 Gaussian noise and uniformly distributed noise

The quantification of NITE is provided in terms of the system parameters and noise standard deviation of σ_n. It is therefore necessary to define the properties of measurement noise. In this section, we cover both Gaussian distributed noise and uniformly distributed noise. Figures 3 (a) and (b) show the characteristics of Gaussian distributed noise and uniformly distributed noise respectively.

When the average value of Gaussian distributed noise is zero, the Gaussian probability density function (pdf) is defined by

$$f(n) = \frac{1}{\sqrt{2\pi}\sigma_n} e^{-\frac{n^2}{2\sigma_n^2}} \tag{2}$$

The Gaussian probability curve shown in Figure 3 (a) describes the noise more prone to occur near zero. The Gaussian probability density function is the famous function most commonly used for the description of noise and random signal sources, because it has convenient properties in all of science and mathematics [18-20]. The Gaussian probability density function is however, not a perfect to explain a realistic noise, because the value of noise variable *n* is infinite.

On the other hand, The uniformly distributed noise follows the uniform probability density function, which limits the value of noise variable *n* to the interval $(-\sigma_n\sqrt{3},\ \sigma_n\sqrt{3})$ and is defined by

$$f(n) = \begin{cases} \frac{1}{2\sigma_n\sqrt{3}} & for\ |n| \le \sigma_n\sqrt{3} \\ 0 & else \end{cases} . \tag{3}$$

The value of noise variable into that interval are equally likely to occur unlike the case of Gaussian distributed noise [21]. Therefore, the uniformly distributed noise is more useful rather than the Gaussian distributed noise if we know the value of noise standard deviation of σ_n exactly.

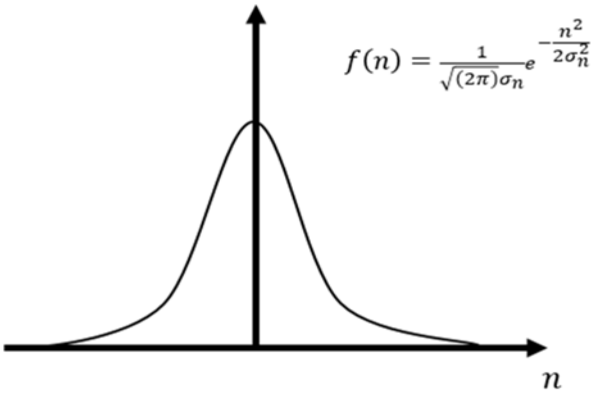

Figure 3 (a). Probability density function of Gaussian distributed noise

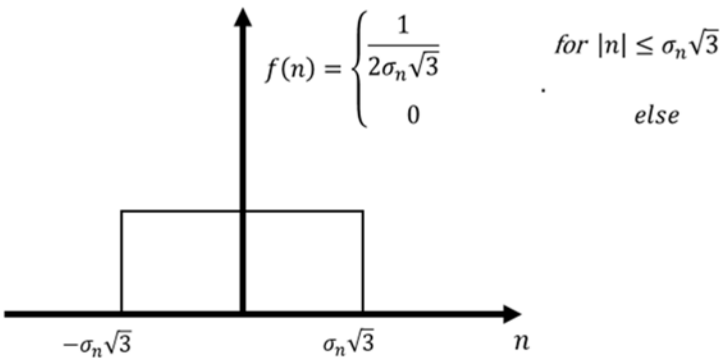

Figure 3 (b). Probability density function of uniformly distributed noise

Ⅲ. Analysis

3.1 Transforming the system using stochastic averaging theory

Before analyzing the PI controlled systems with anti-windups shown in Figures 2 (a), (b), (c), and (d). In order to analyze the systems of Figures 2 (a), (b), (c), and (d), the systems of those can be transformed into that of Figures 4 (a), (b), (c), and (d) respectively. The saturation actuator, $\mathrm{sat}_\alpha^\beta(\mathrm{u})$ is replaced with $h_\alpha^\beta(\bar{u}; K_p\sigma_n)$ by applying stochastic averaging theory [14].

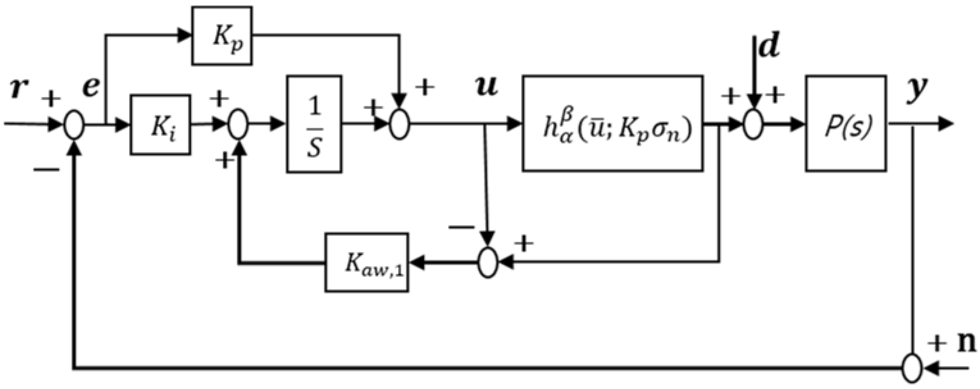

Figure 4 (a). Averaged version of system in Figure 2 (a)

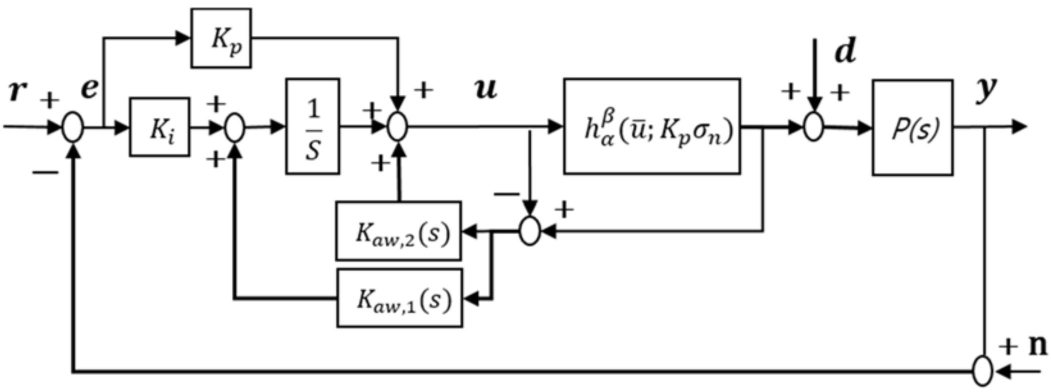

Figure 4 (b). Averaged version of system in Figure 2 (b)

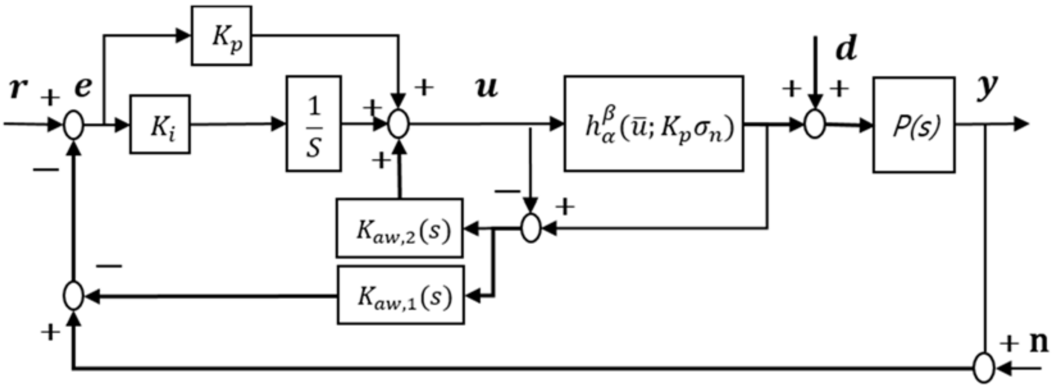

Figure 4 (c). Averaged version of system in Figure 2 (c)

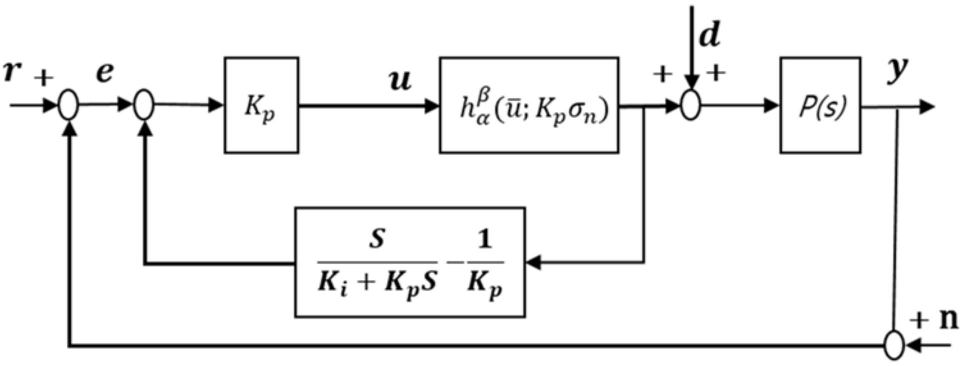

Figure 4 (d). Averaged version of system in Figure 2 (d)

The function $h_\alpha^\beta(\bar{u}; K_p\sigma_n)$ of the systems of Figures 4 (a), (b), (c), and (d) is defined differently depending on distribution characteristics of measurement noise. In the next section, we explain the meaning of the function $h_\alpha^\beta(\bar{u}; K_p\sigma_n)$.

3.1.1 Case 1: Gaussian noise

It is required to define the function $h_\alpha^\beta(\bar{u}; K_p\sigma_n)$ depending on Gaussian distributed noise. When the systems of Figures 2 (a), (b), (c), and (d) have Gaussian distributed noise as shown in Figure 3 (a), the function $h_\alpha^\beta(\bar{u}; K_p\sigma_n)$ is defined as below:

$$h_{g_{\alpha}}^{\beta}(\bar{u};K_p\sigma_n) = \frac{\alpha+\beta}{2} + \frac{\bar{u}-\alpha}{2}\operatorname{erf}\left(\frac{\bar{u}-\alpha}{\sqrt{2}K_p\sigma_n}\right) - \frac{\bar{u}-\beta}{2}\operatorname{erf}\left(\frac{\bar{u}-\beta}{\sqrt{2}K_p\sigma_n}\right) + \frac{K_p\sigma_n}{\sqrt{2\pi}}\left(e^{-\left(\frac{\bar{u}-\alpha}{\sqrt{2}K_p\sigma_n}\right)^2} - e^{\left(\frac{\bar{u}-\beta}{\sqrt{2}K_p\sigma_n}\right)^2}\right) \tag{4}$$

Where, the function $h_{g_{\alpha}}^{\beta}(\bar{u};K_p\sigma_n)$ indicates the function $h_{\alpha}^{\beta}(\bar{u};K_p\sigma_n)$ of the systems of Figures 4 (a), (b), (c), and (d) affected by a Gaussian distributed noise [10]. The function $h_{g_{\alpha}}^{\beta}(\bar{u};K_p\sigma_n)$ is defined as the conditional expected value of $\mathrm{sat}_{\alpha}^{\beta}(u)$ with regard to Gaussian distributed noise n and (4) can be obtained by calculating (5) [10].

$$h_{g_{\alpha}}^{\beta}(\bar{u};K_p\sigma_n) = \int_{-\infty}^{\infty} sat(\bar{u}-K_pn)\frac{1}{\sqrt{2\pi}\sigma_n}e^{-\frac{n^2}{2\sigma_n^2}}dn \tag{5}$$

3.1.2 Case 2: uniformly distributed noise

Similarly, the function $h_{\alpha}^{\beta}(\bar{u};K_p\sigma_n)$ should be defined depending on uniformly distributed noise. When the systems of Figures 2 (a), (b), (c), and (d) have uniformly distributed noise as shown in Figure 3 (b), the function $h_{\alpha}^{\beta}(\bar{u};K_p\sigma_n)$ is defined as below:

1) In case of $\boldsymbol{\sigma_n < \frac{1}{K_p\sqrt{3}}}$

$h_{u_{\alpha}}^{\beta}(\bar{u};K_p\sigma_n)$ is defined by

$$h_{u_\alpha}^{\ \beta}(\bar{u};K_p\sigma_n) = \begin{cases} \alpha & \bar{u} \le \alpha - K_p\sigma_n\sqrt{3} \\ \frac{(\bar{u}+\alpha+K_p\sigma_n\sqrt{3})^2-4\alpha\bar{u}}{2K_p\sigma_n\sqrt{12}} & \alpha - K_p\sigma_n\sqrt{3} < \bar{u} \le \alpha + K_p\sigma_n\sqrt{3} \\ \bar{u} & \alpha + K_p\sigma_n\sqrt{3} < \bar{u} \le \beta - K_p\sigma_n\sqrt{3} \\ \frac{-(\bar{u}+\beta-K_p\sigma_n\sqrt{3})^2+4\beta\bar{u}}{2K_p\sigma_n\sqrt{12}} & \beta - K_p\sigma_n\sqrt{3} < \bar{u} \le \beta + K_p\sigma_n\sqrt{3} \\ \beta & \beta + K_p\sigma_n\sqrt{3} \le \bar{u} \end{cases} \tag{6}$$

2) In case of $\boldsymbol{\sigma_n} \ge \frac{\mathbf{1}}{\boldsymbol{K_p\sqrt{3}}}$

$h_{u_\alpha}^{\ \beta}(\bar{u};K_p\sigma_n)$ is defined by

$$h_{u_\alpha}^{\ \beta}(\bar{u};K_p\sigma_n) = \begin{cases} \alpha & \bar{u} \le \alpha - K_p\sigma_n\sqrt{3} \\ \frac{(\bar{u}+K_p\sigma_n\sqrt{3})^2+\alpha(\alpha-2\bar{u}+2K_p\sigma_n\sqrt{3})}{2K_p\sigma_n\sqrt{12}} & \alpha - K_p\sigma_n\sqrt{3} < \bar{u} \le \beta - K_p\sigma_n\sqrt{3} \\ \frac{\alpha(\alpha-2\bar{u}+2K_p\sigma_n\sqrt{3})-\beta(\beta-2\bar{u}-2K_p\sigma_n\sqrt{3})}{2K_p\sigma_n\sqrt{12}} & \beta - K_p\sigma_n\sqrt{3} < \bar{u} \le \alpha + K_p\sigma_n\sqrt{3} \\ \frac{-(\bar{u}+K_p\sigma_n\sqrt{3})^2-\beta(\beta-2\bar{u}-4K_p\sigma_n\sqrt{3})}{2K_p\sigma_n\sqrt{12}} & \alpha + K_p\sigma_n\sqrt{3} < \bar{u} \le \beta + K_p\sigma_n\sqrt{3} \\ \beta & \beta + K_p\sigma_n\sqrt{3} \le \bar{u} \end{cases} \tag{7}$$

Where, the function $h_{u_\alpha}^{\ \beta}(\bar{u};K_p\sigma_n)$ indicates the function $h_\alpha^\beta(\bar{u};K_p\sigma_n)$ of the systems of Figures 4 (a), (b), (c), and (d) affected by uniformly distributed noise. The function $h_{u_\alpha}^{\ \beta}(\bar{u};K_p\sigma_n)$ is also, defined as the conditional expected value of $\mathrm{sat}_\alpha^\beta(u)$ with regard to uniformly distributed noise n. Both (6) and (7) can be obtained by calculating (8). Unlike the case of Gaussian distributed noise, evaluating integral in (8) gives (6) and (7) depending on the values of the standard deviation of σ_n of measurement noise.

$$h_{u_\alpha}^{\ \beta}(\bar{u};K_p\sigma_n) = \int_{-\sigma_n\sqrt{3}}^{\sigma_n\sqrt{3}} sat(\bar{u}-K_pn)\frac{1}{2\sigma_n\sqrt{3}}dn \tag{8}$$

To compare effects between Gaussian distributed noise and uniformly distributed noise, Figure 5 shows the plot of $h_{g_\alpha}^{\beta}(\bar{u}; K_p\sigma_n)$ and $h_{u_\alpha}^{\beta}(\bar{u}; K_p\sigma_n)$. $\sigma_n = 0.1$ is an arbitrary value that satisfy the condition $\sigma_n < \frac{1}{K_p\sqrt{3}}$ and $\sigma_n = 0.3$ is an arbitrary value that satisfy the condition $\sigma_n \geq \frac{1}{K_p\sqrt{3}}$. The functions $h_{g_\alpha}^{\beta}(\bar{u}; K_p\sigma_n)$ and $h_{u_\alpha}^{\beta}(\bar{u}; K_p\sigma_n)$ are differently determined by noise characteristics.

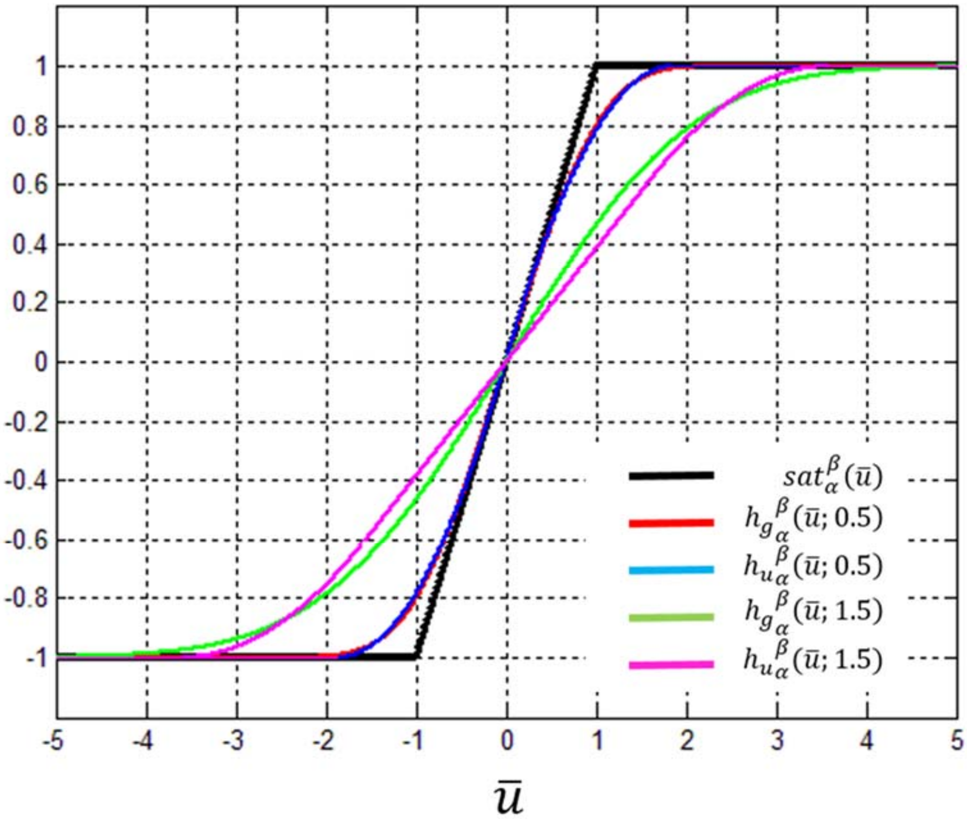

Figure 5. $h_{u_\alpha}^{\beta}(\bar{u}; K_p\sigma_n)$, $h_{g_\alpha}^{\beta}(\bar{u}; K_p\sigma_n)$, and $sat_\alpha^\beta(\bar{u})$ with $\alpha = -1$, $\beta = 1$ for $K_p = 5$, $\sigma_n = 0.1$ and 0.3

3.2 Quantifying NITE

In order to analyze the phenomenon of NITE and figure out the amount of the steady state tracking error, we quantify NITE. Analyzing the systems of Figures 4 (a), (b), (c), and (d) provides the quantification of NITE given in (9). The derivation of (9) is provided in Appendix I.

$$\bar{e}_{ss} = \begin{cases} \dfrac{\left(\bar{u}_{ss} - h_\alpha^\beta(\bar{u}_{ss}; K_p\sigma_n)\right)K_{aw,1}}{K_i} & \text{i)The system of Figure 4 (a)} \\ \dfrac{\left(\bar{u}_{ss} - h_\alpha^\beta(\bar{u}_{ss}; K_p\sigma_n)\right)K_{aw,1}(0)}{K_i} & \text{ii) The system of Figure 4 (b)} \\ \left(\bar{u}_{ss} - h_\alpha^\beta(\bar{u}_{ss}; K_p\sigma_n)\right)K_{aw,1}(0) & \text{iii) The system of Figure 4 (c)} \\ \dfrac{\left(\bar{u}_{ss} - h_\alpha^\beta(\bar{u}_{ss}; K_p\sigma_n)\right)}{K_p} & \text{iv) The system of Figure 4 (d)} \end{cases} \tag{9}$$

Where, $\bar{u}_{ss}$ and $\bar{y}_{ss}$ are respectively, the steady state value of $\bar{u}$ and $\bar{y}$, and $\bar{e}_{ss}$ is the steady state value of tracking error, which indicates the amount of NITE. $K_{aw,1}(0)$ is the d.c gain of $K_{aw,1}$. According to (9), the result on $\bar{e}_{ss}$ gives the conditions under which NITE occurs and we realize that NITE occurs when two conditions must be satisfied at the same time.

The first condition is about measurement noise. According to (9), NITE is never present without measurement noise, regardless of anti-windups. $\bar{u}_{ss} - h_\alpha^\beta(\bar{u}_{ss}; K_p\sigma_n)$ approaches zero as the standard deviation of measurement noise goes to zero because the function $h_\alpha^\beta(\bar{u}; K_p\sigma_n)$ is transformed into $\mathrm{sat}_\alpha^\beta(\bar{u})$. Thus, it can be shown that $\bar{e}_{ss} \approx 0$, which means that NITE hardly exists.

The second condition is about the gains of anti-windup structures. In the systems without anti-windup structures, NITE is not induced by measurement noise. This fact is very clear as you can see in (9). If $K_{aw,1} = 0$ or $K_{aw,1}(0) = 0$, $\bar{e}_{ss} = 0$ regardless of the system parameters and noise characteristics such as integral gain, proportional gain, noise standard deviation, and distribution characteristics of measurement noise. As shown in (9), we figure out that NITE is not caused by $K_{aw,2}(s)$. In other word, anti-windup gains that act as a cause to occur NITE are only $K_{aw,1}$ and $K_{aw,1}(0)$.

Those two conditions show that NITE occurs if both measurement noise and anti-windup exist at the same time regardless of anti-windups. NITE is therefore, likely to occur in all PI controlled systems with anti-windup structures because measurement noise is inevitable.

3.3 Example

In this section, we show that NITE occurs in the PI controlled systems with anti-windup structures shown in Figures 4 (a), (b), (c), and (d) by using MATLAB simulation. The system parameters of Figures 4 (a), (b), (c), and (d) are arbitrarily set to any values that do not make those systems unstable. The system parameters are given in r = 0.9, $K_{AW,1} = 1$, $K_{AW,1}(\mathbf{s}) = \frac{\mathbf{1}}{\boldsymbol{s+1}}$, $K_{AW,2}(\mathbf{s}) = \frac{\mathbf{1}}{\boldsymbol{s+1}}$, K_i= 3, K_p= 5, d=0.01, $P(s) = \frac{2}{5s+2}$. The values of α and β for saturation actuator is -1 and 1 respectively. The simulation results are shown in Figure 5 and Figure 6. The standard deviations of measurement noise are set to $\sigma_n = 0.1$ and $\sigma_n = 0.3$ respectively because the function $h_{u_\alpha}^{\beta}(\bar{u}; K_p\sigma_n)$ is divided into two different definitions depending on the standard deviation of noise. As shown in Figures 6 and Figures 7, the values of $\bar{e}_{ss}$ depends on the standard deviation of measurement noise.

When $\sigma_n = 0.1$, green solid line is the response of the systems of Figures 2 (a), (b), (c), and (d) and red dotted line is the response of the systems of Figures 4 (a), (b), (c), and (d). When $\sigma_n = 0.3$, blue solid line is the response of the systems of Figures 2 (a), (b), (c), and (d) and magenta dotted line is the response of the systems of Figures 4 (a), (b), (c), and (d). The outputs in Figure 6 and Figure 7 are specified as below.

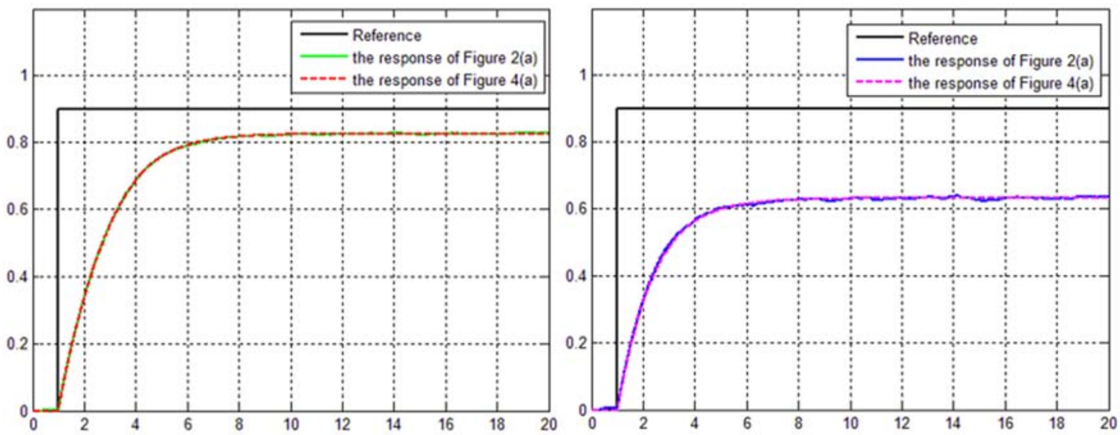

(a) : when $\sigma_n = 0.1$ (left) and $\sigma_n = 0.3$ (right)

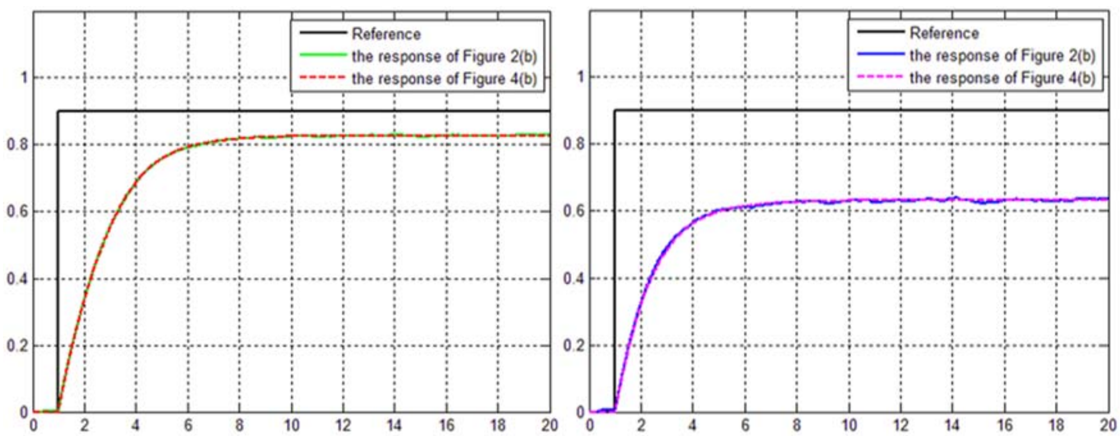

(b) : when $\sigma_n = 0.1$ (left) and $\sigma_n = 0.3$ (right)

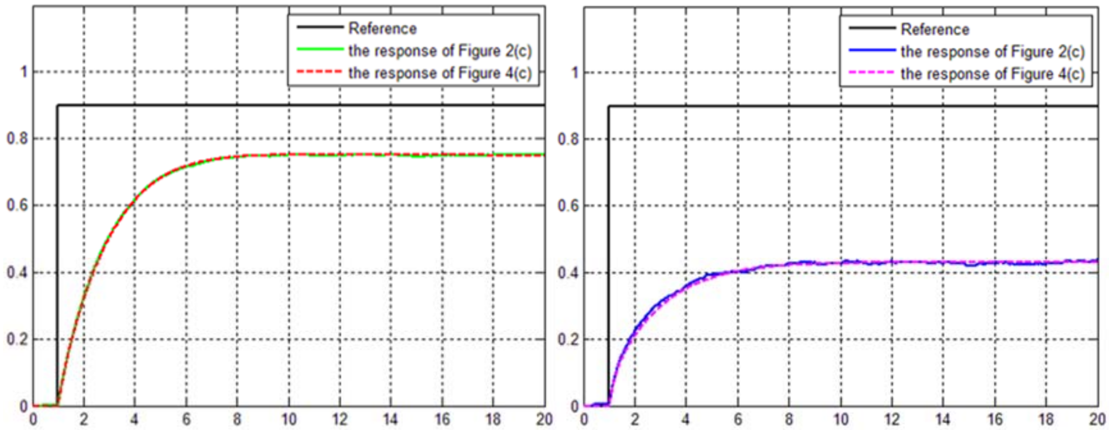

(c) : when $\sigma_n = 0.1$ (left) and $\sigma_n = 0.3$ (right)

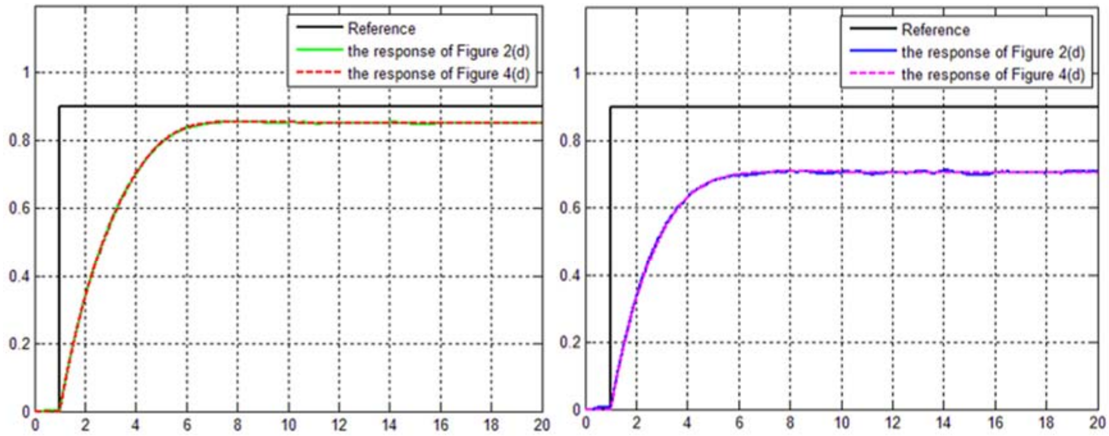

(d) : when $\sigma_n = 0.1$ (left) and $\sigma_n = 0.3$ (right)

Figure 6. The responses of the systems with (a) : Figure 2(a), (b) : Figure 2 (b), (c) : Figure 2 (c) and (d) : Figure 2 (d) under Gaussian noise.

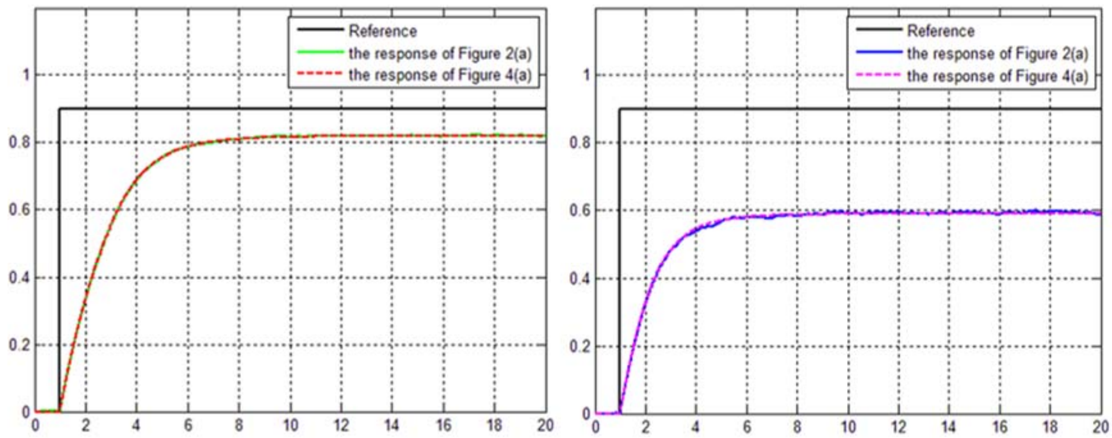

(a) : when $\sigma_n = 0.1$ (left) and $\sigma_n = 0.3$ (right)

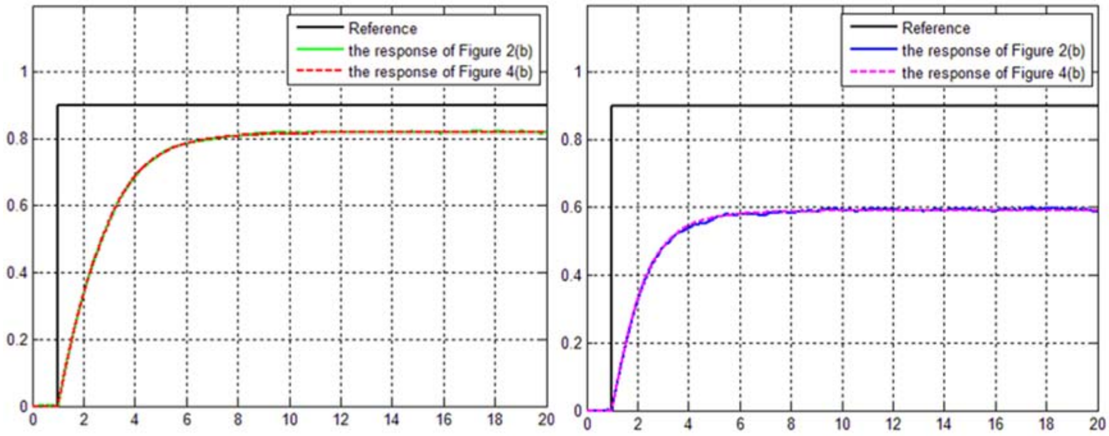

(b) : when $\sigma_n = 0.1$ (left) and $\sigma_n = 0.3$ (right)

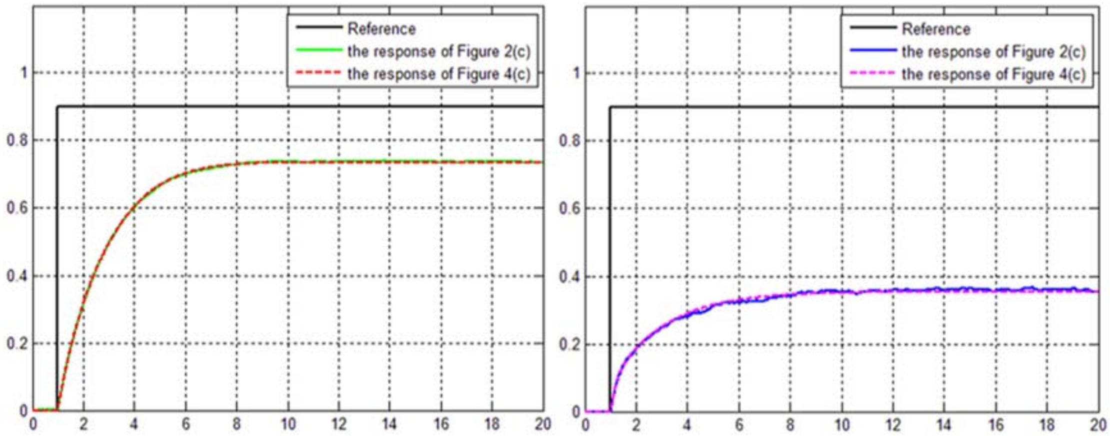

(c) : when $\sigma_n = 0.1$ (left) and $\sigma_n = 0.3$ (right)

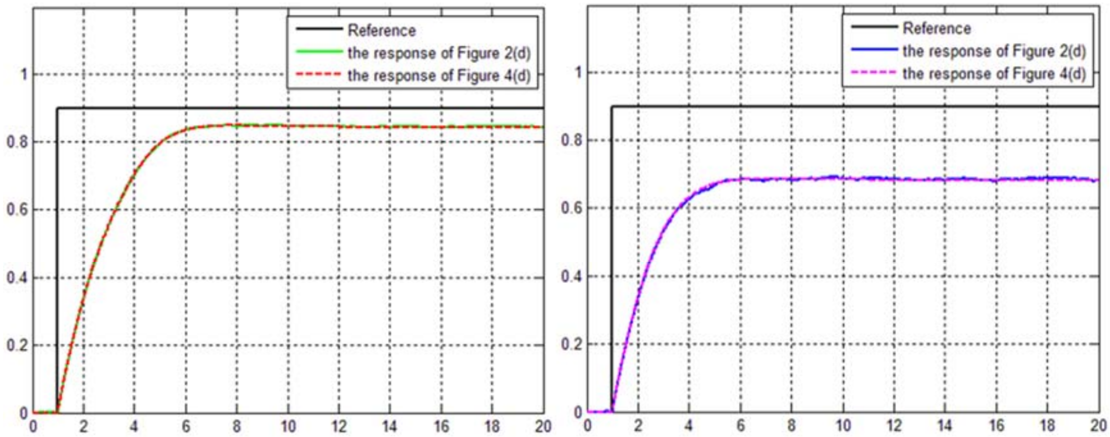

(d) : when $\sigma_n = 0.1$ (left) and $\sigma_n = 0.3$ (right)

Figure 7. The responses of the systems with (a) : Figure 2(a), (b) : Figure 2 (b), (c) : Figure 2 (c) and (d) : Figure 2 (d) under uniformly distributed noise.

These results show that the response of the systems of Figures 2 (a), (b), (c), and (d) are the same with those of Figures 4 (a), (b), (c), and (d). In other word, the systems of Figures 4 shows high accuracy of the analysis method. These results also implies that NITE occurs in all PI controlled systems regardless of anti-windup structures. Thus, the phenomenon of NITE has to be consider significantly in all the industrial systems with anti-windups.

Ⅳ. Solution

4.1 Virtual saturation

The phenomenon of NITE is one of significant issues in all PI controlled systems with anti-windups and it is a problem to be solved. In this section, we suggest two solutions to mitigate the phenomenon of NITE. The First solution is to put another saturation called *virtual saturation* as the input of actual saturation in the systems. In order to avoid the phenomenon of NITE, the virtual saturation has to have bigger saturation bound than actual saturation bound shown in Figures 2. The reason will be referred to section 4.1.1.

The virtual saturation is defined by

$$\mathrm{sat}_{\alpha'}^{\beta'}(u) = \begin{cases} \alpha', & u < \alpha' \\ \beta', & u > \beta' \\ u, & \alpha' \le u \le \beta' \end{cases} \tag{12}$$

Where, u is control input of the virtual saturation and the values of α' and β' should satisfy $\alpha' < \alpha$ and $\beta' > \beta$ respectively.

By putting the virtual saturation, the systems of Figures 2 (a), (b), (c), and (d) can be described in the systems of Figures 8 (a), (b), (c), and (d) respectively. Actual saturation is described in $sat_{\alpha}^{\beta}(sat_{\alpha'}^{\beta'}(u))$ because actual saturation is affected by the virtual saturation $sat_{\alpha'}^{\beta'}(u)$.

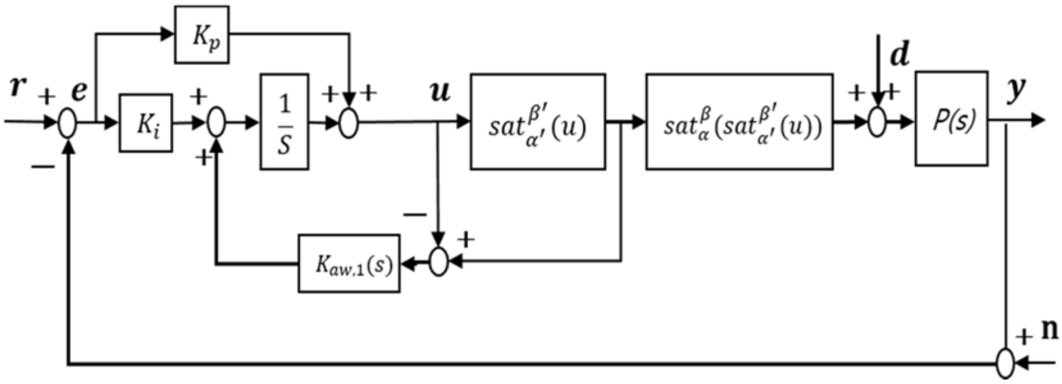

Figure 8 (a). The system of Figure 2 (a) with virtual saturation

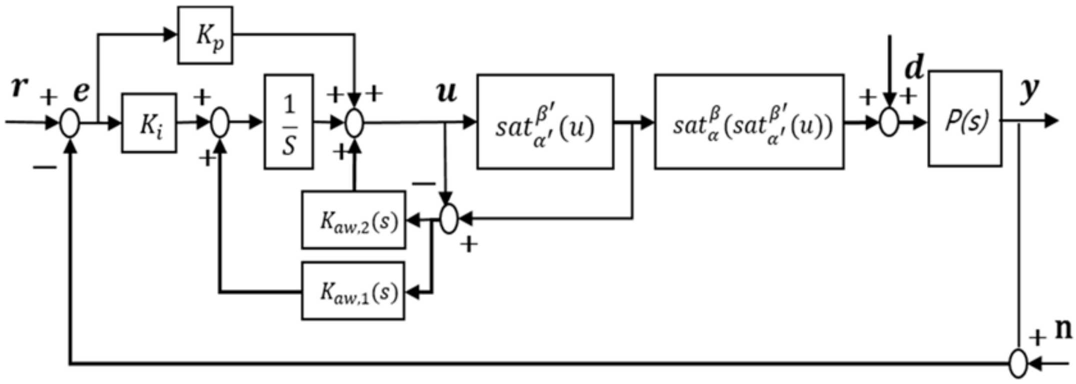

Figure 8 (b). The system of Figure 2 (b) with virtual saturation

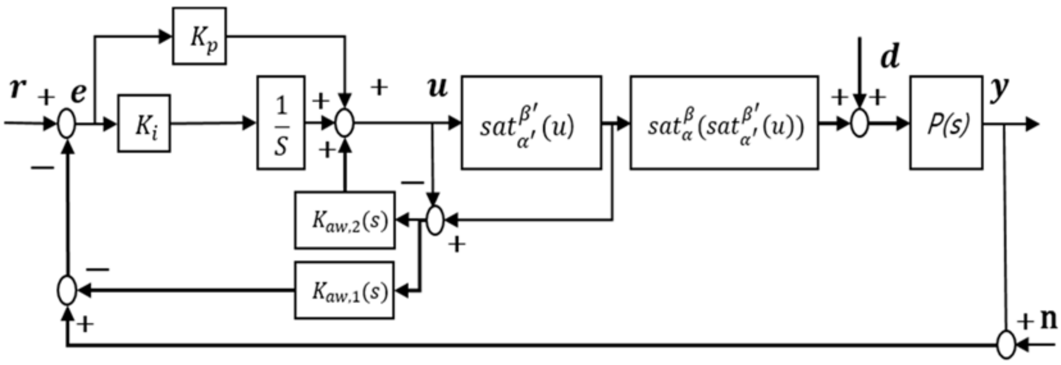

Figure 8 (c). The system of Figure 2 (c) with virtual saturation

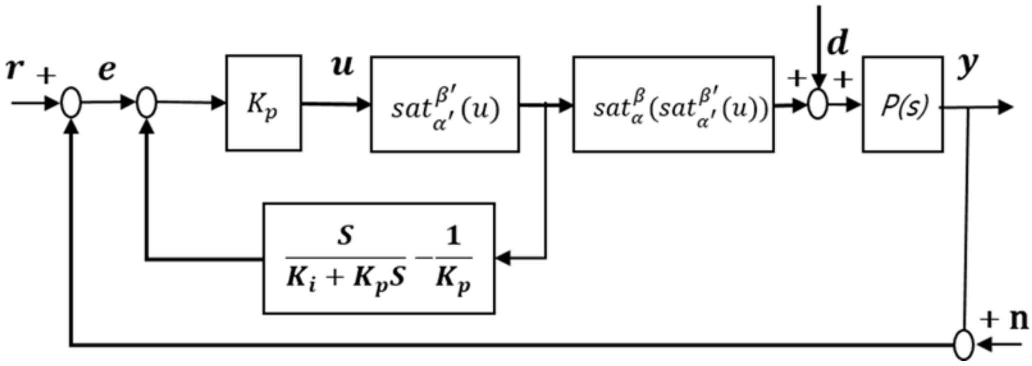

Figure 8 (d). The system of Figure 2 (d) with virtual saturation

In order to figure out how effective the virtual saturation is to prevent the phenomenon of NITE, we quantify the systems of Figures 8 (a), (b), (c), and (d). We transforms the systems of Figures 8 (a), (b), (c), and (d) into the systems of Figures 9 (a), (b), (c), and (d) by applying stochastic averaging theory. The process for this is provided in Appendix II.

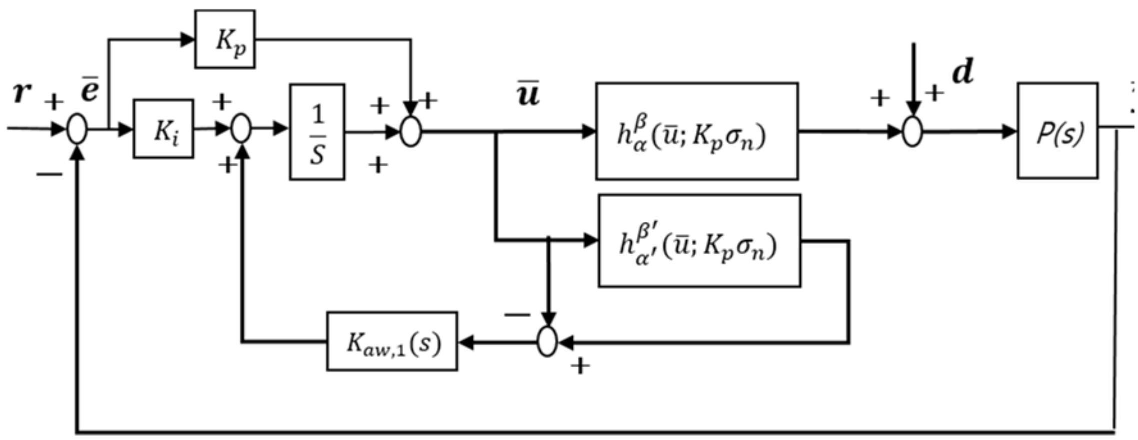

Figure 9 (a). System with virtual saturation equivalent to Figure 8 (a)

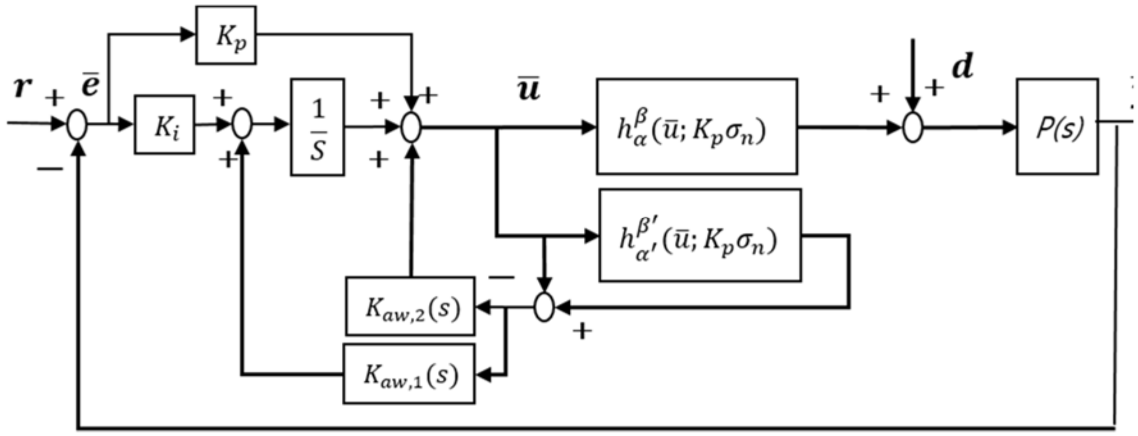

Figure 9 (b). System with virtual saturation equivalent to Figure 8 (b)

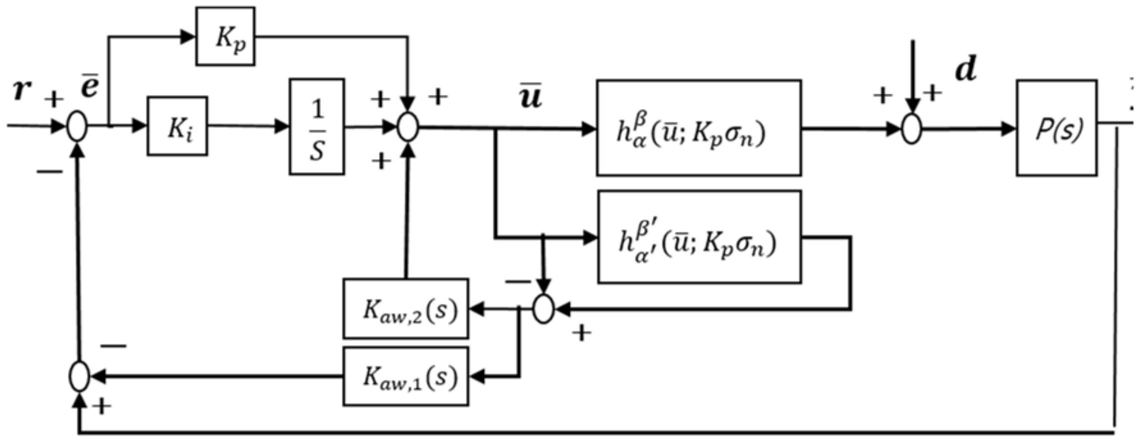

Figure 9 (c). System with virtual saturation equivalent to Figure 8 (c)

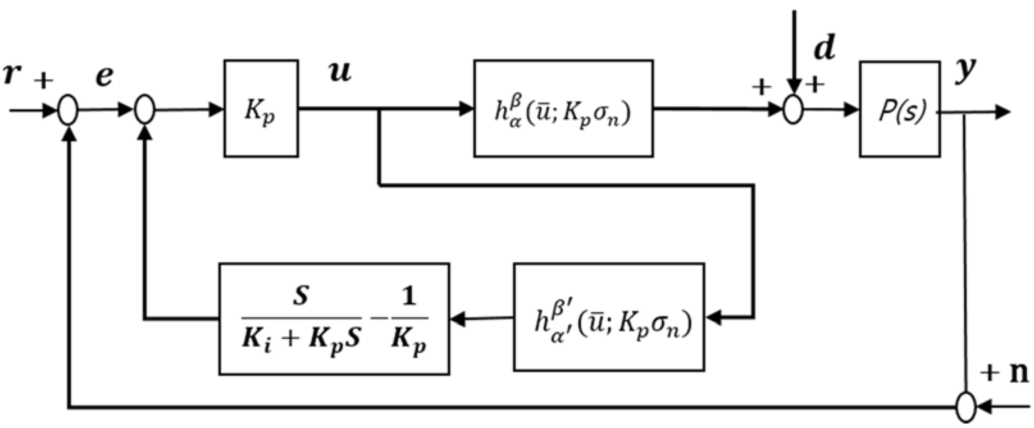

Figure 9 (d). System with virtual saturation equivalent to Figure 8 (d)

As already mentioned through Figures 6 and Figures 7, stochastic averaging theory is reliable method for transforming the systems with respect to measurement noise and the system parameters. The quantification of NITE of the systems of Figures 9 (a), (b), (c), and (d) are defined by

$$\bar{e}_{ss} = \begin{cases} \dfrac{\left(\bar{u}_{ss} - h_{\alpha'}^{\beta'}(\bar{u}_{ss}; K_p\sigma_n)\right) K_{aw,1}}{K_i} & \text{i)The system of Figure 4 (a)} \\ \dfrac{\left(\bar{u}_{ss} - h_{\alpha'}^{\beta'}(\bar{u}_{ss}; K_p\sigma_n)\right) K_{aw,1}(0)}{K_i} & \text{ii) The system of Figure 4 (b)} \\ \left(\bar{u}_{ss} - h_{\alpha'}^{\beta'}(\bar{u}_{ss}; K_p\sigma_n)\right) K_{aw,1}(0) & \text{iii) The system of Figure 4 (c)} \\ \dfrac{\left(\bar{u}_{ss} - h_{\alpha'}^{\beta'}(\bar{u}_{ss}; K_p\sigma_n)\right)}{K_p} & \text{iv) The system of Figure 4 (d)} \end{cases} \tag{13}$$

The derivation of (13) is given in the Appendix III.

The equation of (13) is very similar with (9). Difference are $\bar{u}_{ss}$ and $h_{\alpha'}^{\beta'}(\bar{u}_{ss}; K_p\sigma_n)$. According to (9) and (13), if both integral gain and anti-windup gain of the systems of Figures 9 (a), (b), (c), and (d) are the same with those of the systems of Figures 4 (a), (b), (c), and (d), the amounts of NITE of Figures 4 (a), (b), (c), and (d) are determined by both input and output of actual saturation actuator while the amounts of NITE of Figures 9 (a), (b), (c), and (d) are determined by those of the virtual saturation. In other word, $|\bar{u}_{ss} - h_{\alpha'}^{\beta'}(\bar{u}_{ss}; K_p\sigma_n)|$ should be smaller than that of $|\bar{u}_{ss} - h_{\alpha}^{\beta}(\bar{u}_{ss}; K_p\sigma_n)|$ in order to mitigate NITE. We show that $\bar{u}_{ss} - h_{\alpha'}^{\beta'}(\bar{u}_{ss}; K_p\sigma_n)$ is smaller than $\bar{u}_{ss} - h_{\alpha}^{\beta}(\bar{u}_{ss}; K_p\sigma_n)$ in Appendix V.

As shown in (13), the virtual saturation provides clue to reduce NITE. We therefore, need to determine the values of both α' and β' in order to reduce NITE. In the next section, we determine the values of both α' and β'.

4.1.1 Virtual saturation limit

In this section, we determine the values of the virtual saturation bound α' and β' in order to mitigate NITE. According to (13), $\bar{e}_{ss}$ is small if $\bar{u}_{ss} - h_{\alpha'}^{\beta'}(\bar{u}_{ss}; K_p\sigma_n)$ small. That is, $\bar{u}_{ss}$ is in the region where $\bar{u} \approx h_{\alpha'}^{\beta'}(\bar{u}; K_p\sigma_n)$. As plot of such region, Figure 10 shows the Function $h_{\alpha'}^{\beta'}(\bar{u}; K_p\sigma_n)$

along with $sat_{\alpha'}^{\beta'}(\bar{u})$. There exists a region of $\bar{u}$ where $h_{\alpha'}^{\beta'}(\bar{u}; K_p\sigma_n)$ and $\bar{u}$ are almost identical. As shown in Figure 10, the region can be characterized by two inequalities of (14) and (15).

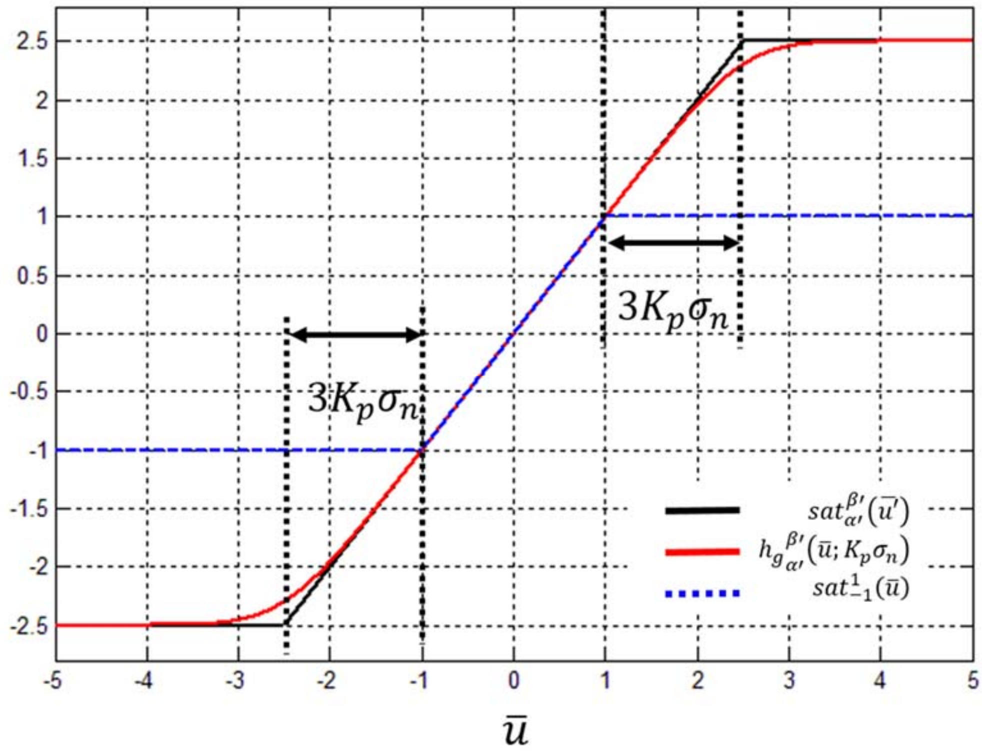

Figure 10. Plot of $sat_{\alpha'}^{\beta'}(\bar{u})$, $sat_{-1}^{1}(\bar{u})$, and $h_{g_{\alpha'}}^{\beta'}(\bar{u}; K_p\sigma_n)$ under Gaussian distributed noise

$$\bar{u} - \alpha' > 3K_p\sigma_n \tag{14}$$

$$\beta' - \bar{u} > 3K_p\sigma_n \tag{15}$$

Where, the margin of $3K_p\sigma_n$ is determined using the Gaussian distributed noise and is useful range to prevent anti-windup activation from measurement noise. That is, $\bar{u}$ remains in the linear region, and doesn't activate the anti-windups with a probability larger than 0.99 because approximately 99% of the values from Gaussian distributed noise are within $3K_p$.

According to (14) and (15), $\bar{e}_{ss}$ goes to zero because of $\bar{u} \approx h_{\alpha'}^{\beta'}(\bar{u}; K_p\sigma_n)$. That is, NITE can be avoided when α' and β' satisfy the range of $\alpha' \leq \alpha - 3K_p\sigma_n$ and $\beta' \geq \beta + 3K_p\sigma_n$. This fact can be applied to the systems under uniformly distributed noise. Figure 11 indicates the systems of Figure 9 under uniformly distributed noise.

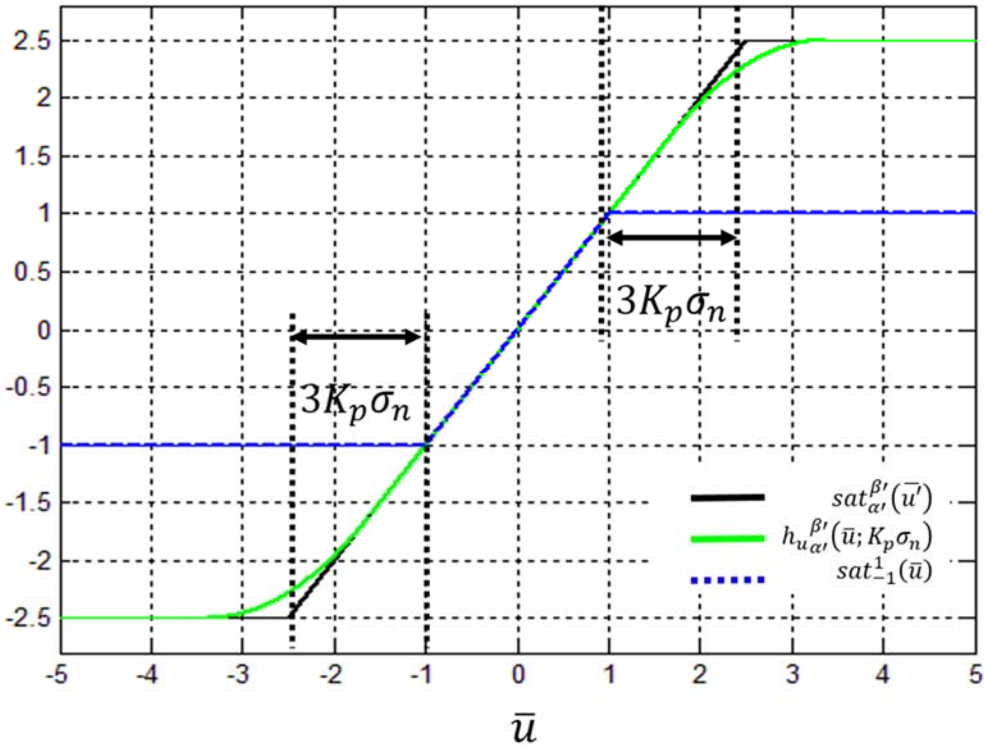

Figure 11. Plot of $sat_{\alpha'}^{\beta'}(\bar{u})$, $sat_{-1}^{1}(\bar{u})$, and $h_{g_{\alpha'}}^{\beta'}(\bar{u}; K_p\sigma_n)$ under uniformly distributed noise

4.1.2 Stability based on LMI

In order to show the stability of PI controlled systems with virtual saturation, we analyze the stability of the systems with virtual saturation by using Linear matrix inequalities (LMI). LMI techniques have been especially, used to determine the stability of linear systems subject to actuator saturation. We here, show the internal stability of the system of Figure 8(a) with static full authority anti-windup strategy, which is the same as back-calculation anti-windup due to the algebraic loop in here.

The state space forms of the system of Figure 8(a) is shown as below.

$$\begin{aligned} \dot{x}_p &= A_p x_p + B_p sat_2(u) \\ y_p &= C_p x_p \\ u &= K_p(-y_p) + x_i \\ \dot{x}_i &= K_i(-y_p) + K_{aw,1}(sat_1(u) - u) \end{aligned} \tag{16}$$

Here, x_p, x_i, u, and y_p are the state of the plant, the state of the integral controller, the control input, and the output of the plant respectively. $sat_1(u)$ is a virtual saturation and $sat_2(u)$ is a actual saturation actuator.

We introduce the deadzone nonlinearity to arrive at LMI when checking the internal stability of the systems with saturation actuator. The basic idea is to inscribe the saturation or deadzone into a conic region (the space between the two red-dotted lines) shown in Figure 12. The left side of Figure 12 is the graph of the saturation function and the deadzone nonlinear is shown in the right side of Figure 12. The graph of saturation function is contained in a conic sector and the deadzone nonlinearity is contained in this sector. We utilize the deadzone nonlinearity, because it doesn't degrade the system performance and is useful to express LMI technique. This sector has the property that its output *y* always the same sign as its input *u* and the amount of *y* is not bigger than that of *u* [22-23].

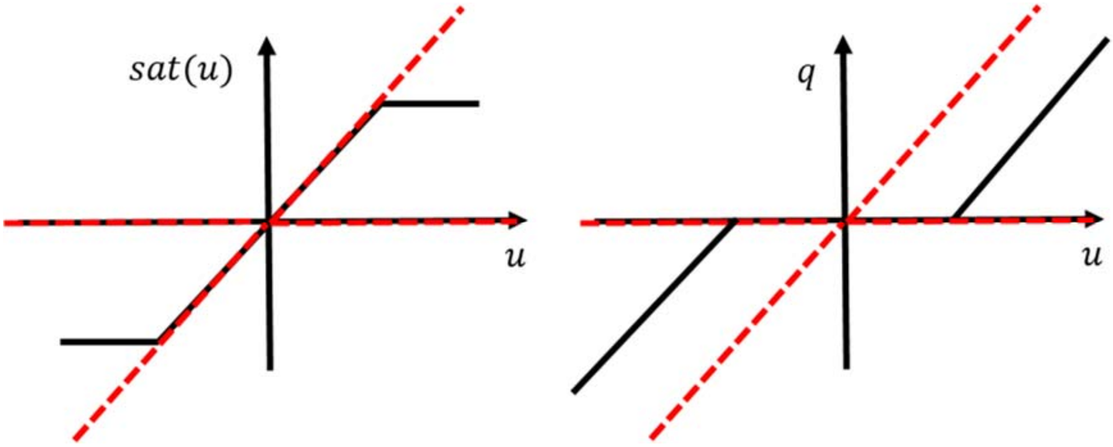

Figure 12. The saturation function(left) and the deadzone function (right)

Here, the output of deadzone function of actual saturation and that of virtual saturation are referred to as q_1 and q_2 respectively. The output of deadzone function is defined by

$$\begin{aligned} q_1 &= u - sat_1(u) \\ q_2 &= sat_1(u) - sat_2(u) \end{aligned} \tag{17}$$

This sector can be mathematically expressed using inequality $y(u-y) \geq 0$, which becomes $q(u-q) \geq 0$ in case of the deadzone nonlinearity where $y = q$.
In case of vector deadzone nonlinearity, $q(u-q)$ can be written as

$$q_1^T W_1 (u - q_1) \geq 0 \tag{18}$$

$$q_2^T W_2 (u - q_1 - q_2) \geq 0 \tag{19}$$

Where W_1 and W_2 are a diagonal matrix which consists of arbitrary positive weighting. (18) is the deadzone nonlinearity of virtual saturation and (19) is that of actual saturation.
According to (16) and (17), the state space form of the system of Figure 8 (a) is written as

$$\begin{gathered} \dot{x}_p = (A_p - B_p K_p C_p) x_p + B_p x_i - B_p q' - B_p q \\ y_p = C_p x_p \\ \dot{x}_i = -K_i C_p x_p - K_{aw,1} q' \\ u = -K_p C_p x_p + x_i \end{gathered} \tag{20}$$

By selecting $x = \begin{bmatrix} x_p^T & x_i^T \end{bmatrix}^T$ and $q = [q_1{}^T \quad q_2{}^T]^T$, (16) is rewritten in the form of linear matrix inequalities as below

$$\begin{gathered} \dot{x} = Ax + Bq \\ \mathrm{u} = Cx \end{gathered} \tag{21}$$

where, $A = \begin{bmatrix} A_p - B_p K_p C_p & B_p \\ -K_i C_p & 0 \end{bmatrix}$, $B = [B_1 \;\; B_2] = \begin{bmatrix} -B_p & -B_p \\ -K_{aw,1} & 0 \end{bmatrix}$, $C = [-K_i C_p \quad 1]$

By depending on quadratic Lyapunov function $V = x^T P x$ with $P > 0$, it is desirable for the time derivative of V to be negative except at the origin. The time derivative can be determined from the directional derivative of V in the direction $Ax + Bq$, which is provided by [12],[23]

$$\dot{V} = x^T(A^T P + PA)x + 2x^T PBq < 0 \tag{22}$$

The nonlinear elements is required to consider the sector conditions in (18) and (19). Therefore, we can use the following sufficient condition to guarantee (22):

$$x^T(A^T P + PA)x + 2x^T PBq + 2q_1^T W_1(u - q_1) + 2q_2^T W_2(u - q_2) \tag{23}$$

This inequality (23) can be rewritten as

$$\begin{pmatrix} A^T P + PA & C^T W_1 + PB_1 & PB_2 + C^T W_2 \\ W_1 C + B_1^T P & -2W_1 & -W_2 \\ B_2^T P + W_2 C & -W_2 & -2W_2 \end{pmatrix} < 0 \tag{24}$$

If the above LMI is feasible, then the system with virtual saturation is said to be internally stable. In other words, there exist the free variables P, which satisfy the condition in (24).
Although the Internal Stability is determined by technique based on LMI, both virtual saturation bound and actual saturation bound have to be considered in order to guarantee the internal stability.

4.2 Dynamic P gain

In PI controlled systems, Proportional gain block of PI controller is commonly static, which means the block with no memory, while the proportional gain block is said to be dynamic if the block has memory. Changing the proportional gain block into dynamic is helpful to mitigate NITE and we call the dynamic block *dynamic P gain*. Figures 13 (a), (b), (c), and (d) show the systems containing dynamic P gain with anti-windups.

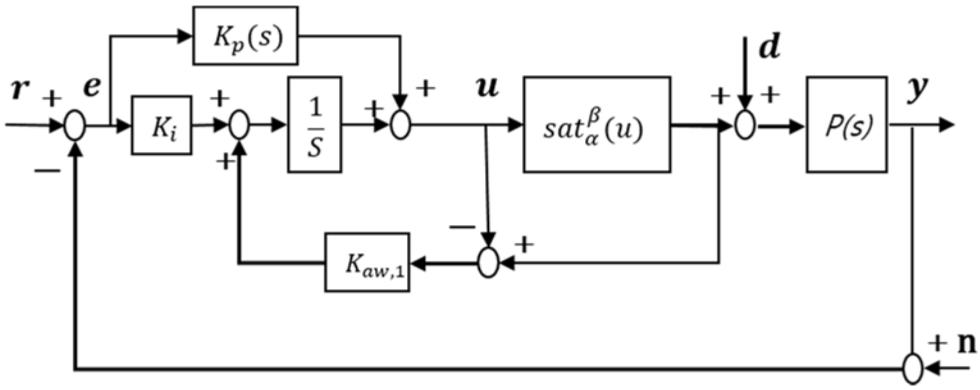

Figure 13 (a). Block diagram of the system of Figure 2 (a) with dynamic P gain controller

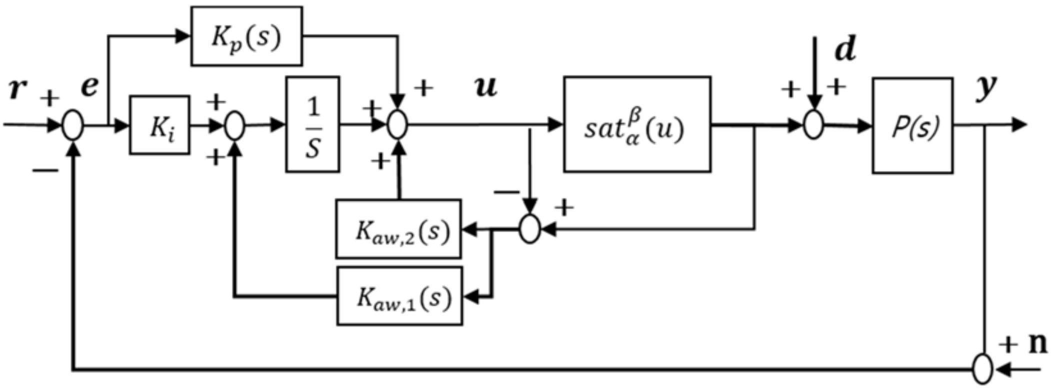

Figure 13 (b). Block diagram of the system of Figure 2 (b) with dynamic P gain controller

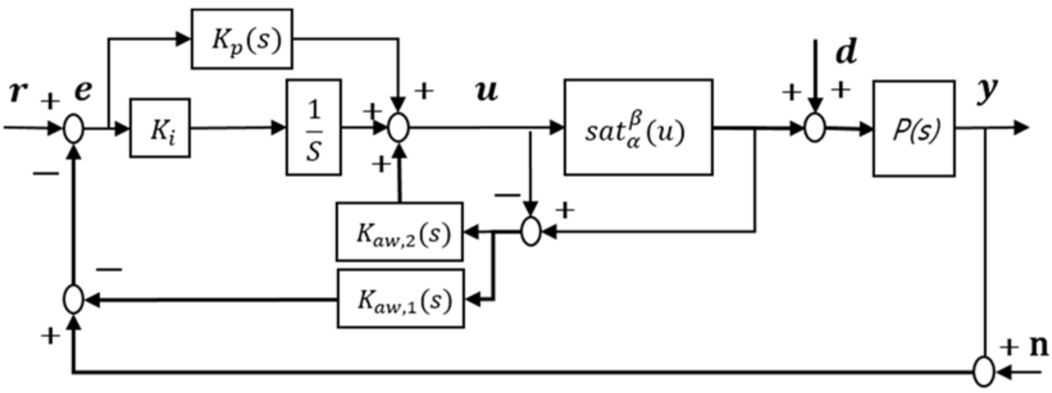

Figure 13 (c). Block diagram of the system of Figure 2 (c) with dynamic P gain controller

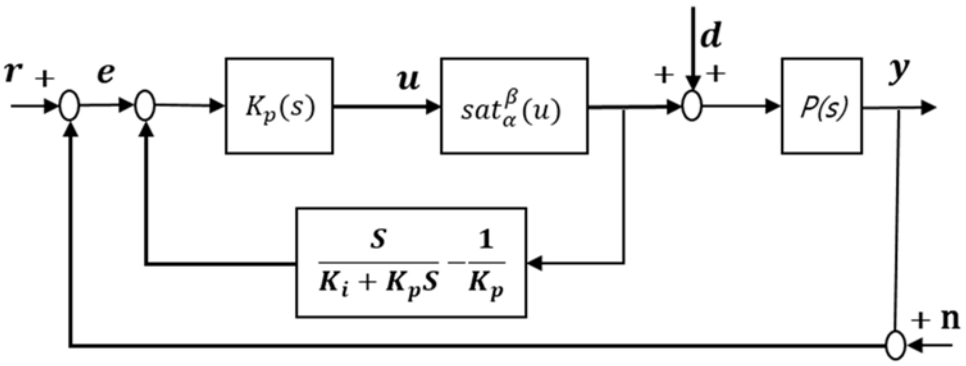

Figure 13 (d). Block diagram of the system of Figure 2 (d) with dynamic P gain controller

Figures 13 (a), (b), (c), and (d) are respectively, PI controlled systems similar with Figures 2 (a), (b), (c), and (d). The only difference between Figures 13 and Figures 2 is the proportional gain of PI controller. Actually, although the controller in Figures 13 is not PI controller anymore because the proportional gain is not static, the controller in Figures 13 acts as PI controller which has the role of eliminating tracking error in systems.

By applying stochastic averaging theory, the systems of Figures 13 (a), (b), (c), and (d) are respectively, transformed to the averaged systems of Figures 14 (a), (b), (c), and (d). The averaged systems is used to quantify NITE, so we can check whether NITE occurs or not.

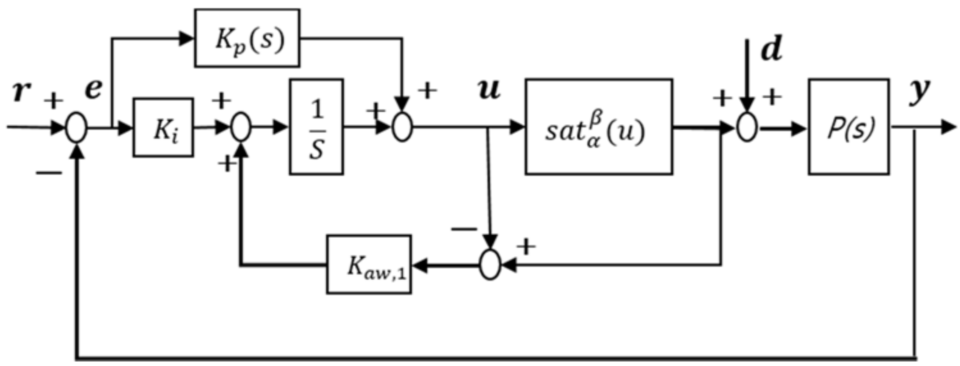

Figure 14 (a). Averaged version of system in Figure 13 (a).

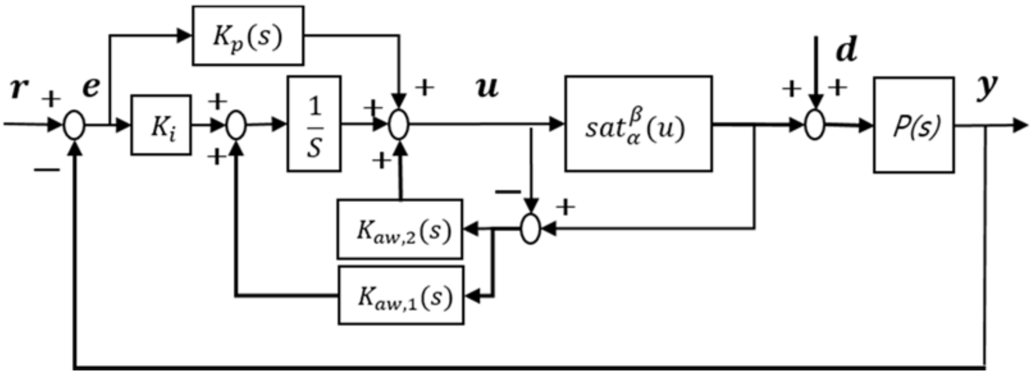

Figure 14 (b). Averaged version of system in Figure 13 (b)

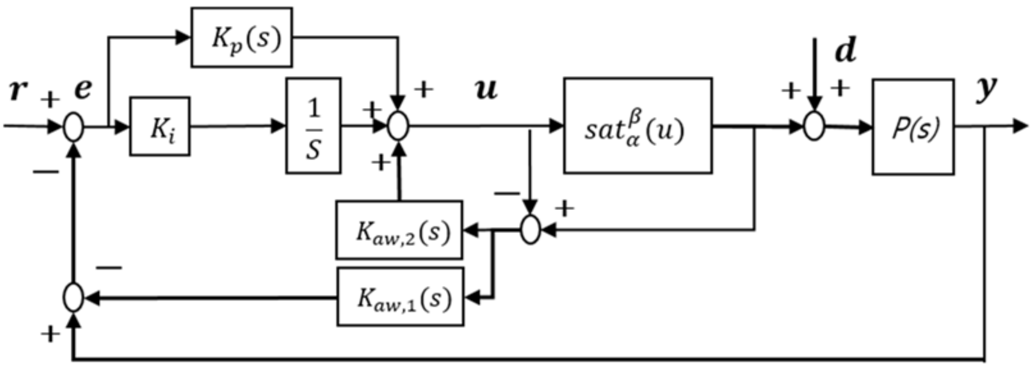

Figure 14 (c). Averaged version of system in Figure 13 (c)

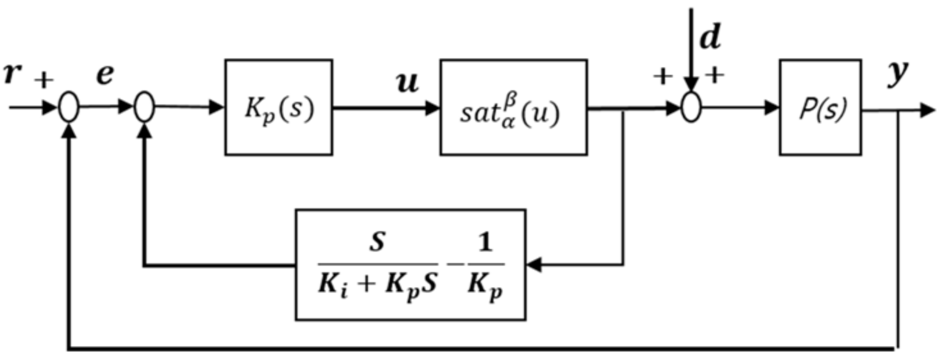

Figure 14 (d). Averaged version of system in Figure 13 (d)

However, there is a difference here between the systems of Figures 14 and Figures 4. Generally, function $h_\alpha^\beta(\bar{u}; K_p\sigma_n)$ is substituted for the saturation nonlinearity by applying stochastic averaging theory, but the saturation nonlinearity of the systems of Figures 14 is defined as $\mathrm{sat}_\alpha^\beta(\bar{u})$ instead of

$h_{\alpha}^{\beta}(\bar{u}; K_p\sigma_n)$. It means that noise does not affect to the saturation nonlinearity. The reason for this is proved in Appendix V.

According to (9), NITE exists due to a gap between $\bar{u}$ and $h_{\alpha}^{\beta}(\bar{u}; K_p\sigma_n)$. In other words, $\bar{e}_{ss}$ is zero because a gap between $\bar{u}$ and $\mathrm{sat}_{\alpha}^{\beta}(\bar{u})$ does not exist. Consequently, NITE does not occur in the systems of Figures 14. We shows the results of the systems of Figures 14 in the next section.

4.3 Result

We suggest two methods to mitigate NITE so far. In this section, we show that the results of the systems of both Figures 9 and Figures 14 and compare the results of the systems of Figures 9 with that of Figures 14. The systems parameters of both Figures 9 and Figures 14 are referred to [10] and given in Table 1.

Table 1. Simulation parameters in the systems of Figures 9 and Figures 14

	The systems of Figure 9	The systems of Figure 14
K_i	3	3
K_p	5	5
$K_{aw,1}$	1	1
$K_{aw,2}(s)$	$\frac{1}{s+1}$	$\frac{1}{s+1}$
$K_{aw,1}(s)$	$\frac{1}{s+1}$	$\frac{1}{s+1}$
β'	2.5	Not applicable
α'	-2.5	Not applicable
β	1	1
α	-1	-1
$P(s)$	$\frac{2}{5s+2}$	$\frac{2}{5s+2}$
σ_n	0.1	0.1
$K_p(s)$	Not applicable	$\frac{5}{s+1}$

The parameters of α' and β' is determined based on section 4.1.1. The parameter of $K_p(s)$ is decided arbitrary without making the stability of the systems of Figures 14 unstable. Using the parameters in Table 1, The simulation is carried out and the results are shown in below.

Figure 15 is the response of the systems of Figures 9 (a), (b), (c), and (d) under Gaussian distributed noise. Figure 16 is the response of the systems of Figures 9 (a), (b), (c), and (d) under uniformly distributed noise.

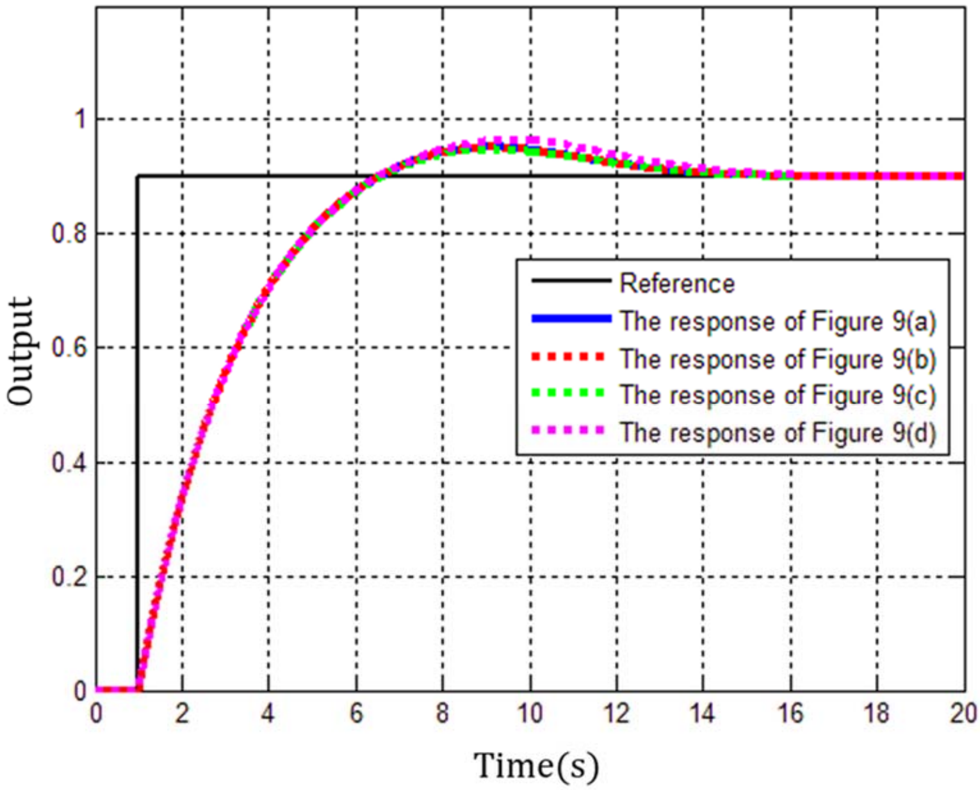

Figure 15. The responses of the systems of Figures 9 under Gaussian distributed noise

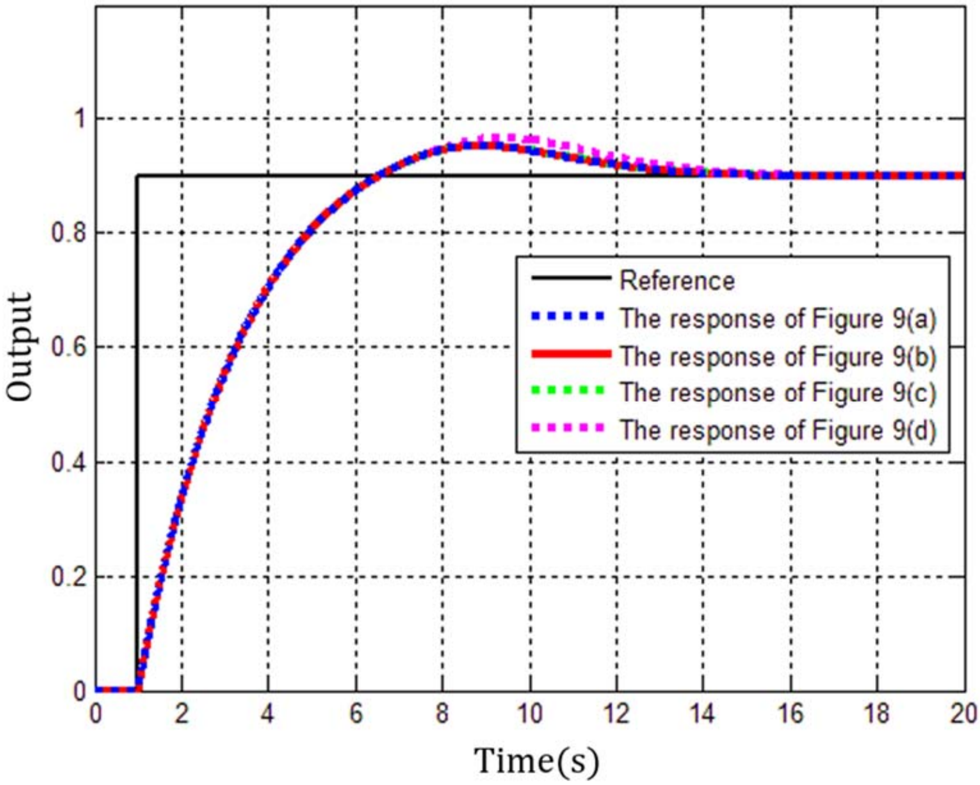

Figure 16. The responses of the systems of Figures 9 under uniformly distributed noise

As the results of the Figures 15 and Figures 16, putting virtual saturation in the system with anti-windups mitigates the phenomenon of NITE. In comparison with the outputs of the systems of Figures 4, the steady state tracking errors of Figures 9 (a), (b), (c), and (d) are smaller than that of Figures 4 (a), (b), (c), and (d) respectively. It means that NITE hardly exists in the systems of Figures 9 (a), (b), (c), and (d).

Figure 17 shows the responses of the systems of Figures 14 (a), (b), (c), and (d), which mean the controlled systems containing dynamic P gain.

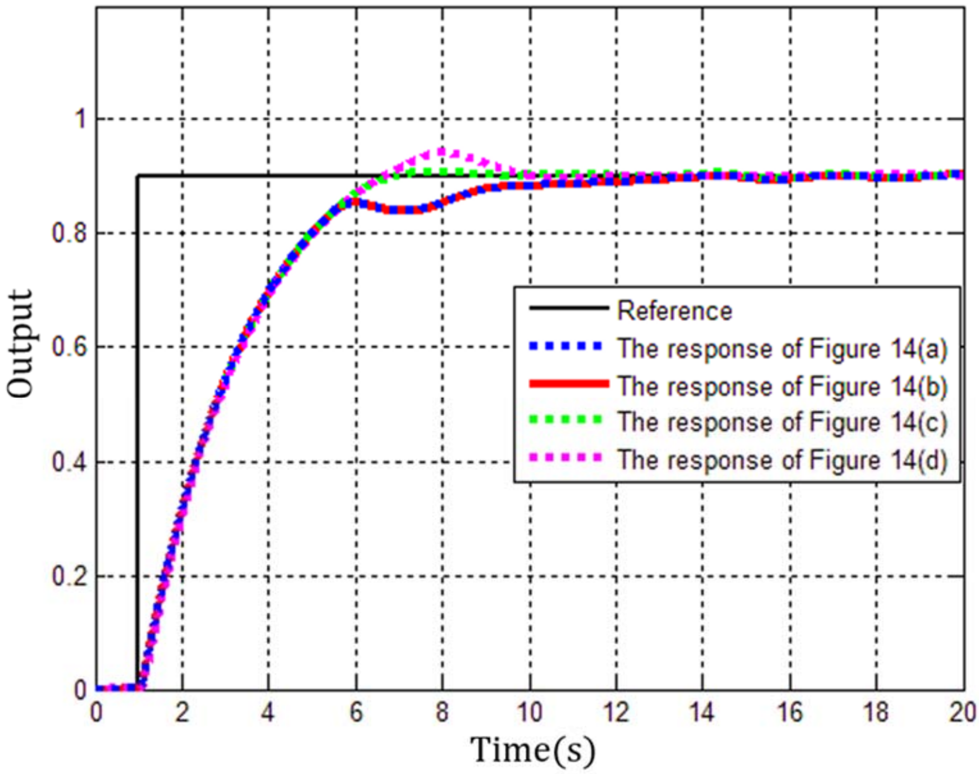

Figure 17. The responses of the systems of Figures 14

Like the systems of Figures 9 (a), (b), (c), and (d), Figure 17 indicates that NITE can be avoided in the systems of Figures 14 (a), (b), (c), and (d). The outputs of the systems of Figure 14 (a), (b), (c), and (d) are 0.9 because the saturation actuator $\mathrm{sat}_{\alpha}^{\beta}(\bar{u})$ in the systems of Figure 14 (a), (b), (c), and (d) are not replaced with $h_{\alpha}^{\beta}(\bar{u}; K_p\sigma_n)$ despite applying stochastic averaging theory. That is, $\bar{e}_{ss}$ of the systems of Figures 14 (a), (b), (c), and (d) are all zero.

Two above mentioned solutions are useful methods to prevent the phenomenon of NITE, but they have different characteristics as in shown Figures 15, 16, and 17.

i) The overshoot of the systems of Figures 9 (a), (b), (c), and (d) are generally bigger than that of Figure 14 (a), (b), (c), and (d).

ii) There are a little oscillations of the systems of Figures 14 (a) and (b) unlike the response of the systems of Figured 9 (a) and (b)

iii) Without measurement noise, anti-windup effect become weaker in the systems of Figures 9, which cause the overshoot.

Ⅴ. Application

5.1 Electro-active polymer

The phenomenon of NITE was originally discovered in toner concentration control of digital printing [10]. Besides the toner concentration control, NITE could occur most of all PI controlled systems in industrial applications. One example is electro-active polymer (EAP). The EAP is a kind of materials made up of polymers, metals, and other elements that show unique properties. The EAP can be used to produce a mechanical motion depending on electric voltage and utilized as a sensor by measuring the output voltage generated by imposed mechanical deformation [24].

Through this application, precision position control of the EAP actuator is shown by using a digital PID controller with an integrator anti-windup structure that prevent performance degradation due to saturation nonlinearity. Figure 18 is a diagram of the EAP actuator system in order to show working principle of the EAP actuator. A working principle of the EAP actuator is a simple. When the EAP actuator is affected by an electric field, the total charge inside the EAP strip actuator in response to the electric field causes the bending motion [24].

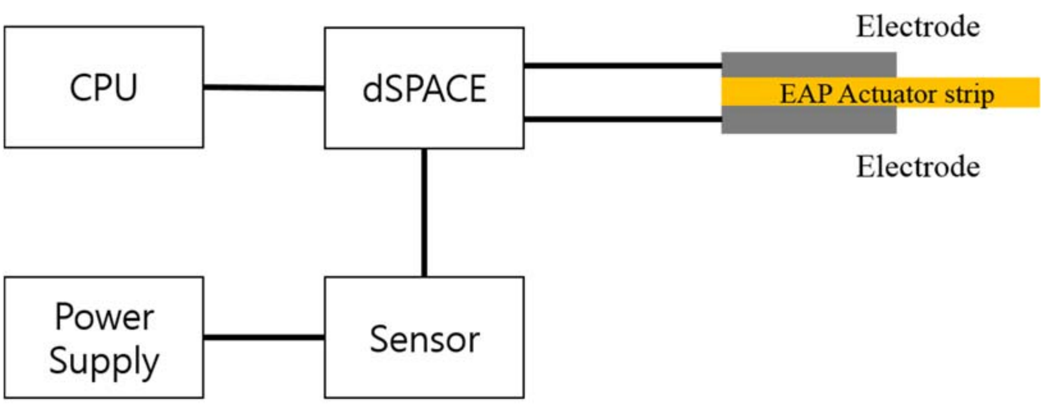

Figure 18. A diagram of the experimental setup.

Here, dSPACE contains 16-bit analogue to digital (A/D) converter channel of a digital-signal-processing (DSP) board. Details are referred to [24].

Figure 19 show a block diagram for the closed-loop digital position control of the EAP actuator with an integrator anti-windup scheme. The parameters of the system of Figure 19 is provided in [24]. We assume that measurement noise is Gaussian distributed noise of which standard deviation of σ_n set to 0.3.

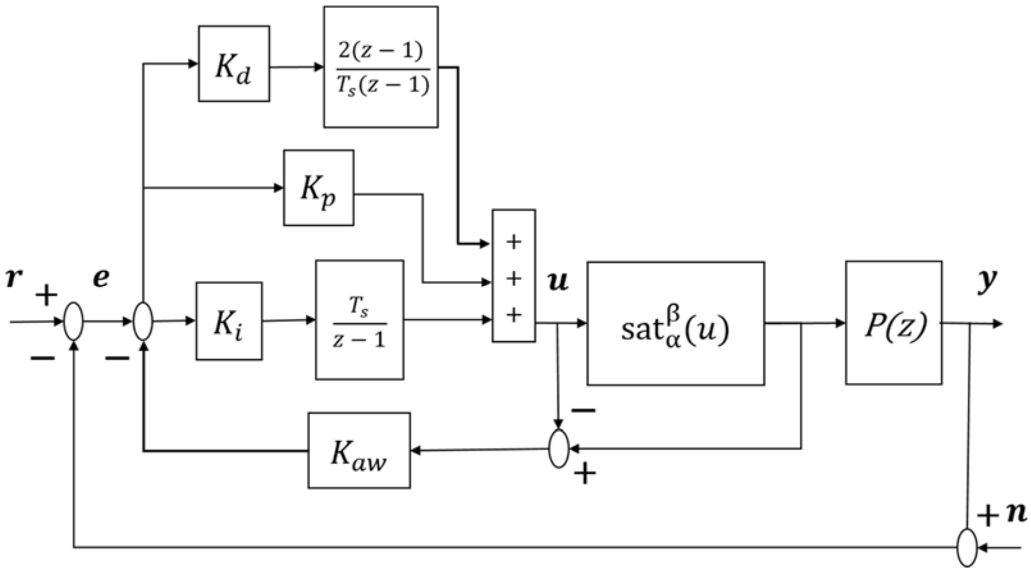

Figure 19. A block diagram of the closed-loop position control of the EAP actuator.

Simulation result of the EAP actuator is shown in Figure 20. The black line indicates a 0.8 mm reference of the system of Figure 19 and the red line presents a step response of the system of Figure 19. As presented in Figure 20, the phenomenon of NITE could occurs in the EAP actuator system. This result means that NITE is very significant issue to most of all controlled systems with anti-windup.

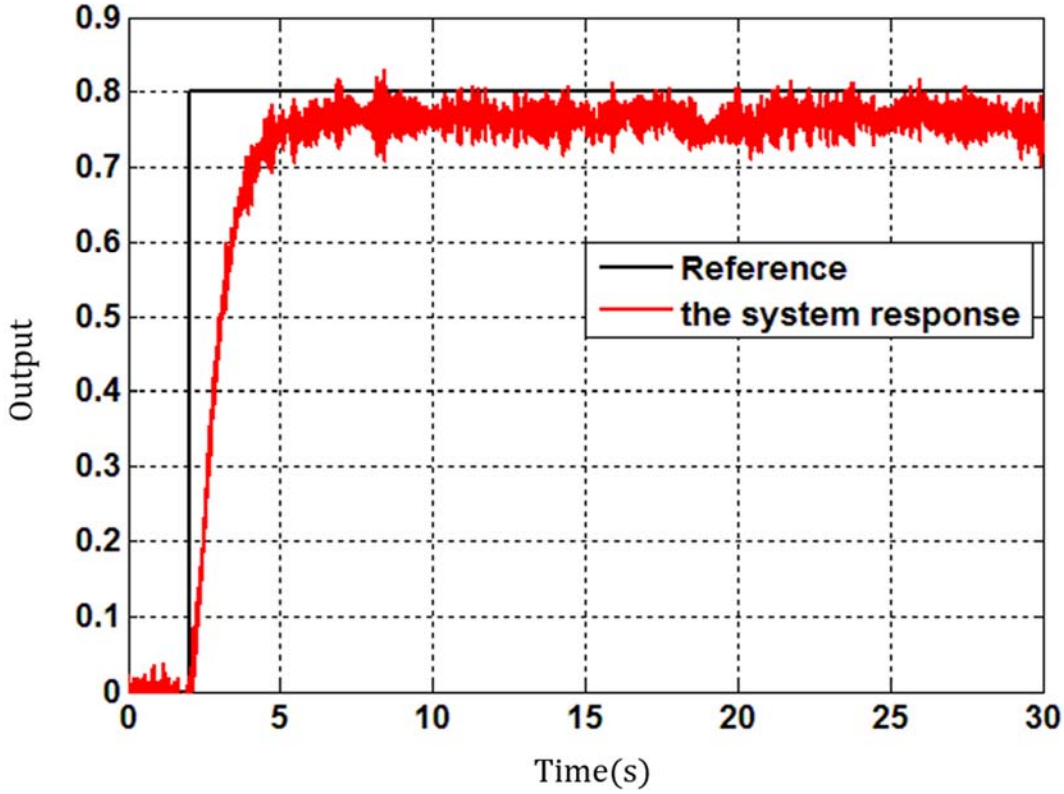

Figure 20. Simulation result of the position control of EAP actuator under Gaussian distributed noise

5.2 Applying the solutions in the system

We have suggested two solutions in this paper. One solution is called *virtual saturation* and the other solution is called *dynamic P gain*. Virtual saturation affects saturation actuator by increasing range in the input of saturation actuator, While dynamic P gain affects proportional gain of PI controller by changing static proportional gain to dynamic one. Figure 21 (a) shows the position control system of EAP actuator with virtual saturation and Figure 21 (b) shows the system applying the dynamic P gain. According to (12) and (13), the values of α' and β' are respectively, set to -1 and 1. $\frac{0.004K_p}{z-0.996}$ is the block of dynamic P gain. K_p is the same value of the position control system of the EAP actuator in [24].

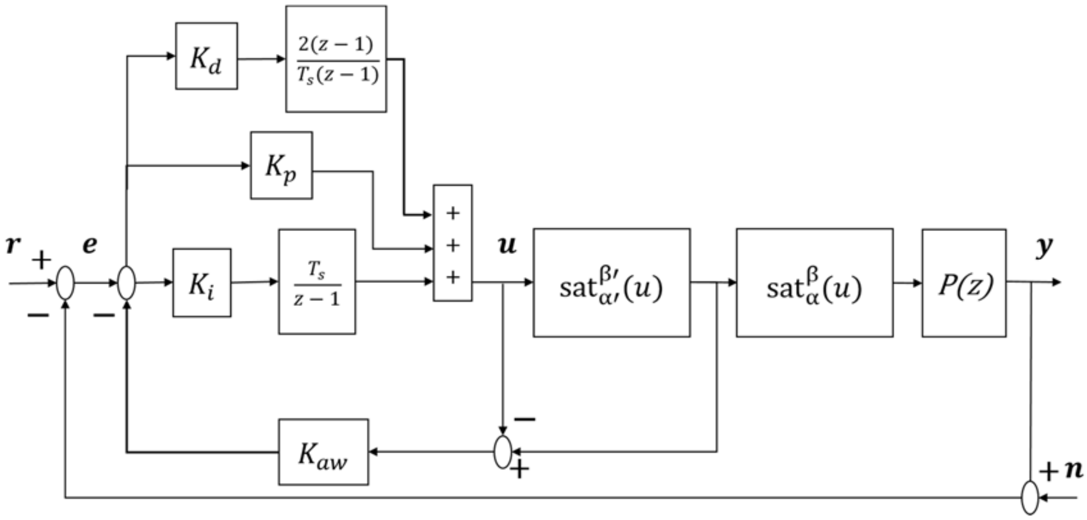

Figure 21 (a). A block diagram of the position control system of the EAP actuator with virtual saturation.

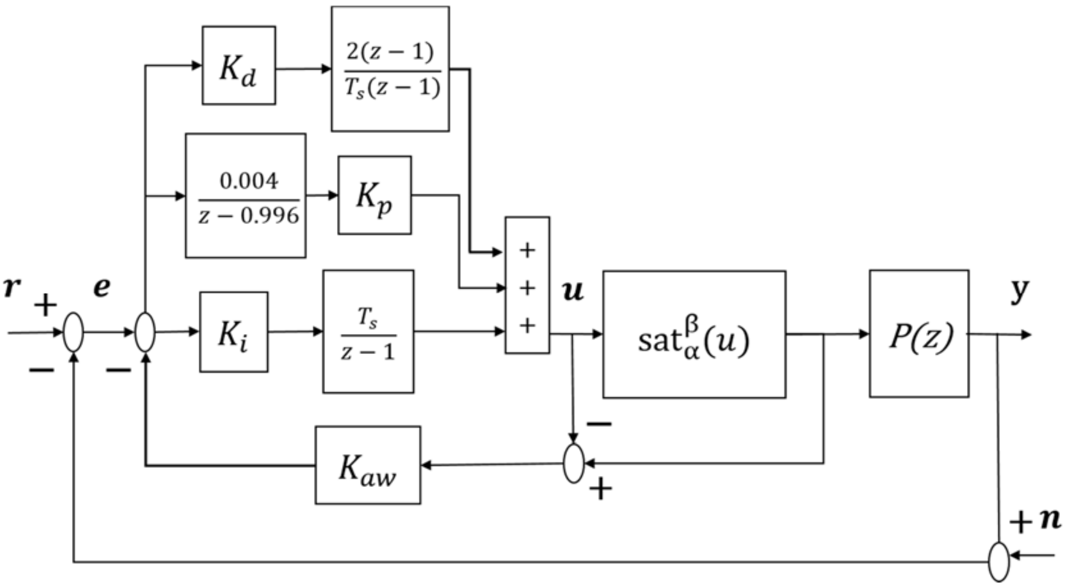

Figure 21 (b). A block diagram of the position control system of the EAP actuator with dynamic P gain.

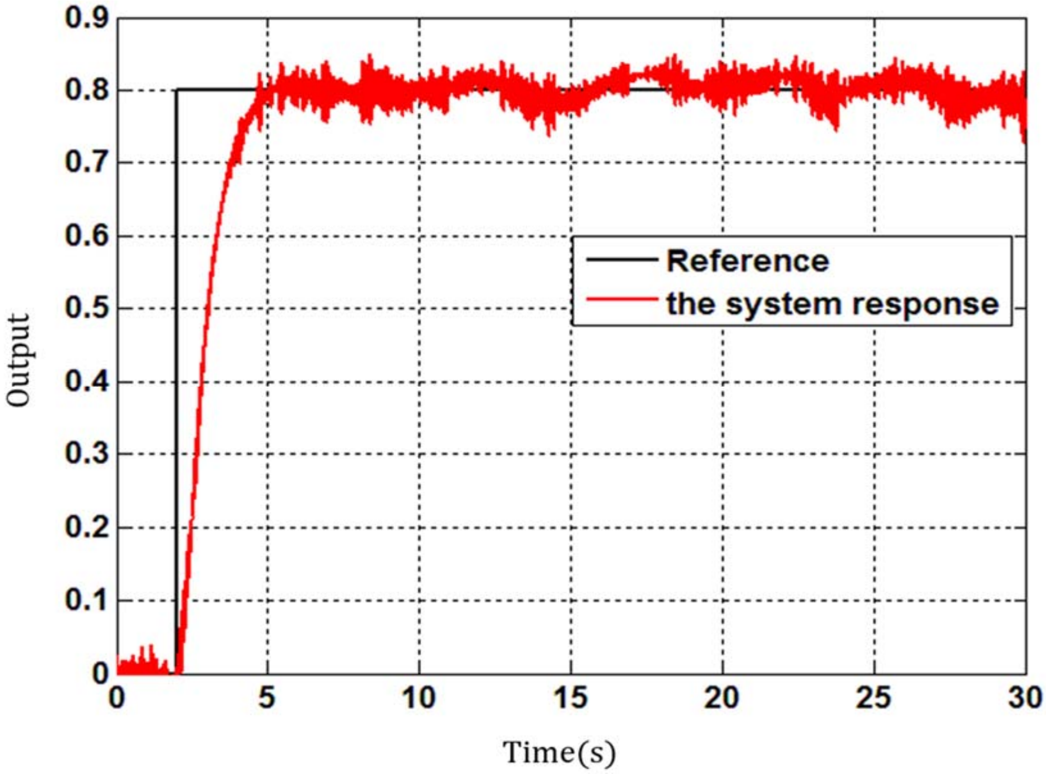

Figure 22 (a). The response of the system of Figure 21 (a)

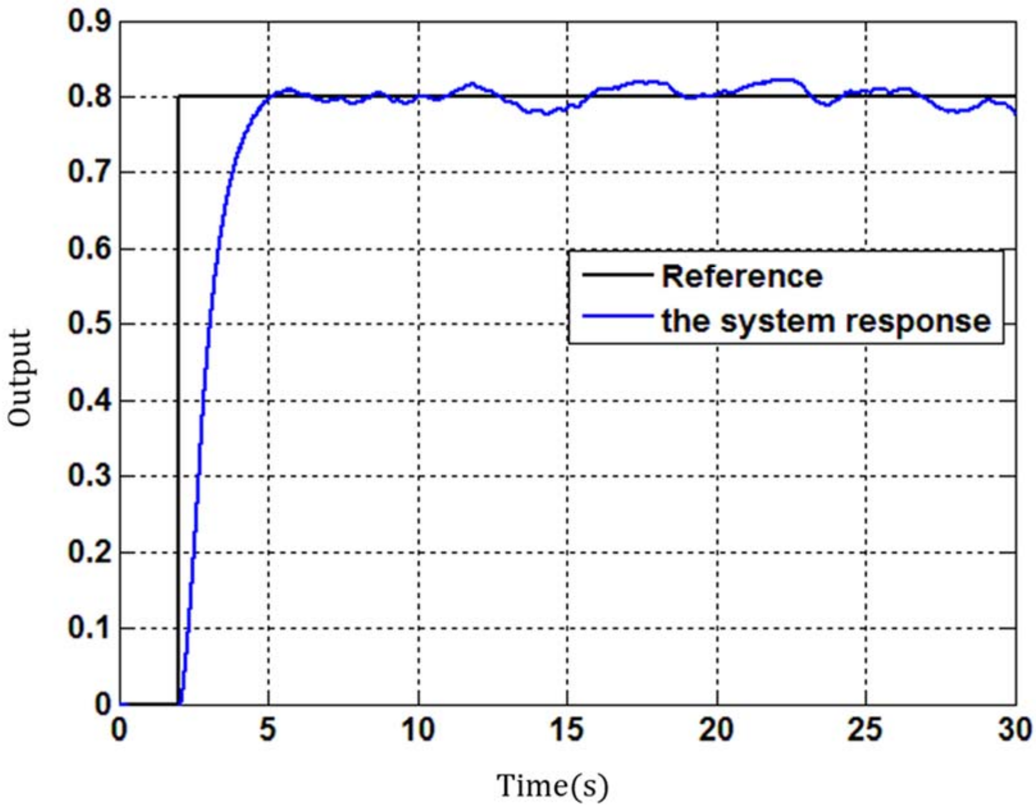

Figure 22 (b). The response of The system of Figure 21 (b)

The effects of both virtual saturation and dynamic P gain are demonstrated in Figure 22. The red line is the response of the position control system of the EAP actuator of Figure 21 (a). The blue line indicates the response of Figure 21 (b). As you can see, both of methods are effective solutions to mitigate NITE. By applying the stochastic averaging, it is possible to analyze NITE of the EAP position control system. However, we didn’t deal with it because the EAP position control system is described as discrete system.

Ⅵ. Conclusion

Recently, In PI controlled systems with anti-windup called back-calculation, steady state tracking error due to measurement noise has been reported and this steady state tracking error was named NITE. In this study, we showed that Noise induced tracking error (NITE) could occur in all PI controlled systems with anti-windup structures as well. In other words, NITE could occur in all the systems if both anti-windup and measurement noise exist, regardless of anti-windups.

Using stochastic averaging theory, we quantified the noise induced tracking error in terms of system parameters and noise characteristics, and showed that NITE occurred with uniformly distributed noise as well as Gaussian distributed noise

We suggested two solutions to mitigate NITE. One method is using Virtual saturation, which act as the input of actual saturation and has bound bigger than actual saturation has. We analyzed how virtual saturation affect to the systems likely to NITE. An analysis of internal stability based on linear matrix inequalities was conducted on the system with two saturation actuators. The other method is changing static P gain to dynamic P gain. We checked that dynamic P gain played the role of eliminating an effect of noise in the systems.

Ⅶ. Appendix Ⅰ

i) The system of Figure 4 (a) (PI controlled system with back-calculation anti-windup)

Let the state space realization of the system of Figure 4 (a) be

$$\begin{aligned} \dot{\bar{x}}_p &= A_p\bar{x}_p + B_p h_\alpha^\beta(\bar{u}; K_p\sigma_n) + B_p d \\ \dot{\bar{x}}_i &= K_i(r-\bar{y}) + K_{aw,1}\left(h_\alpha^\beta(\bar{u}; K_p\sigma_n) - \bar{u}\right) \\ \bar{y} &= C_\mathrm{p}\bar{x}_p \\ u &= K_p(r-\bar{y}) + \bar{x}_i \end{aligned} \tag{25}$$

Where, $\bar{x}_p$, $\bar{x}_i$, $\bar{u}$, d, and $\bar{y}$, and are the state of the plant, the state of the integral controller, the control input, the disturbance of the system and the output of the system of Figure 4 (a) respectively.
The steady state of this system is defined by

$$\begin{aligned} 0 &= A_p\bar{x}_p + B_p h_\alpha^\beta(\bar{u}; K_p\sigma_n) + B_p d \\ 0 &= K_i(r-\bar{y}) + K_{aw,1}\left(h_\alpha^\beta(\bar{u}; K_p\sigma_n) - \bar{u}\right) \end{aligned} \tag{26}$$

Assuming that the asymptotically stable equilibrium exists

$$0 = K_i(r-\bar{y}_{ss}) + K_{aw,1}\left(h_\alpha^\beta(\bar{u}_{ss}; K_p\sigma_n) - \bar{u}_{ss}\right) \tag{27}$$

Should be satisfied in the steady state, where $\bar{y}_{ss}$ and $\bar{u}_{ss}$ are the steady state values of $\bar{y}$ and $\bar{u}$.
Therefore, $\bar{e}_{ss}$ is defined as below

$$\bar{e}_{ss} = r - \bar{y}_{ss} = \frac{K_{aw,1}}{K_i}\left(\bar{u}_{ss} - h_\alpha^\beta(\bar{u}_{ss}; K_p\sigma_n)\right) \tag{28}$$

ii) The system of Figure 4 (b) (PI controlled system with dynamic static full authority anti-windup)

Let the state space realization of the system of Figure 4 (b) be

$$
\begin{gathered}
\dot{\bar{x}}_p = A_p \bar{x}_p + B_p h_\alpha^\beta(\bar{u}; K_p\sigma_n) + B_p d \\
\bar{y} = C_\mathrm{p} \bar{x}_p \\
\dot{\bar{x}}_{aw,1} = A_{aw,1}\bar{x}_{aw,1} + B_{aw.1}\left(h_\alpha^\beta(\bar{u}; K_p\sigma_n) - \bar{u}\right) \\
\bar{y}_{aw,1} = C_{\mathrm{aw},1}\bar{x}_{aw,1} \\
\dot{\bar{x}}_{aw,2} = A_{aw,2}\bar{x}_{aw,2} + B_{aw.2}\left(h_\alpha^\beta(\bar{u}; K_p\sigma_n) - \bar{u}\right) \\
\bar{y}_{aw,2} = C_{\mathrm{aw},2}\bar{x}_{aw,2} \\
\dot{\bar{x}}_i = K_i(r - \bar{y}) + C_{\mathrm{aw},1}\bar{x}_{aw,1} \\
\bar{u} = K_p(r - \bar{y}) + \bar{x}_i + C_{\mathrm{aw},2}\bar{x}_{aw,2}
\end{gathered} \tag{29}
$$

Where, $\bar{x}_{aw,1}$ and $\bar{x}_{aw,2}$ are the state space form of the dynamic anti-windup gain $K_{aw,1}(s)$ and $K_{aw,2}(s)$ respectively. The steady state of this system is defined by

$$
\begin{gathered}
0 = A_p \bar{x}_p + B_p h_\alpha^\beta(\bar{u}; K_p\sigma_n) + B_p d \\
0 = A_{aw,1}\bar{x}_{aw,1} + B_{aw.1}\left(h_\alpha^\beta(\bar{u}; K_p\sigma_n) - \bar{u}\right) \\
0 = A_{aw,2}\bar{x}_{aw,2} + B_{aw.2}\left(h_\alpha^\beta(\bar{u}; K_p\sigma_n) - \bar{u}\right) \\
0 = K_i(r - \bar{y}) + C_{\mathrm{aw},1}\bar{x}_{aw,1}
\end{gathered} \tag{30}
$$

Assuming that the asymptotically stable equilibrium exists

$$
\begin{gathered}
0 = K_i(r - \bar{y}_{ss}) + C_{\mathrm{aw},1}\bar{x}_{aw,1} \\
0 = A_{aw,1}\bar{x}_{aw,1} + B_{aw.1}\left(h_\alpha^\beta(\bar{u}_{ss}; K_p\sigma_n) - \bar{u}_{ss}\right) \\
\bar{y}_{aw,1} = C_{\mathrm{aw},1}\bar{x}_{aw,1}
\end{gathered} \tag{31}
$$

According to (31), $\bar{y}_{aw,1}$ is written as below

$$
\bar{y}_{aw,1} = -\mathrm{C}_{\mathrm{aw},1}A_{aw,1}^{-1}\mathrm{B}_{\mathrm{aw},1}\left(-\bar{u}_{ss} + h_\alpha^\beta(\bar{u}_{ss}; K_p\sigma_n)\right) = K_{aw,1}(0)\left(\bar{u}_{ss} - h_\alpha^\beta(\bar{u}_{ss}; K_p\sigma_n)\right) \tag{32}
$$

Where, $K_{aw,1}(0)$ is dc gain of the anti-windup gain $K_{aw,1}(s)$. Replacing $C_{\mathrm{aw},1}\bar{x}_{aw,1}$ with (32), $\bar{e}_{ss}$ can be defined as below

$$
\bar{e}_{ss} = r - \bar{y}_{ss} = \frac{K_{aw,1}(0)}{K_i}\left(\bar{u}_{ss} - h_\alpha^\beta(\bar{u}_{ss}; K_p\sigma_n)\right) \tag{33}
$$

iii) The system of Figure 4 (c) (PI controlled system with dynamic external global anti-windup)

The state space form is as below

$$\begin{gathered}
\dot{\bar{x}}_p = A_p \bar{x}_p + B_p h_\alpha^\beta(\bar{u}; K_p \sigma_n) + B_p d \\
\bar{y} = C_\mathrm{p} \bar{x}_p \\
\dot{\bar{x}}_{aw,1} = A_{aw,1} \bar{x}_{aw,1} + B_{aw.1}\left(h_\alpha^\beta(\bar{u}; K_p \sigma_n) - \bar{u}\right) \\
\bar{y}_{aw,1} = C_{\mathrm{aw},1} \bar{x}_{aw,1} \\
\dot{\bar{x}}_{aw,2} = A_{aw,2} \bar{x}_{aw,2} + B_{aw.2}\left(h_\alpha^\beta(\bar{u}; K_p \sigma_n) - \bar{u}\right) \\
\bar{y}_{aw,2} = C_{\mathrm{aw},2} \bar{x}_{aw,2} \\
\dot{\bar{x}}_i = K_i\left(r - \bar{y} + C_{\mathrm{aw},1} \bar{x}_{aw,1}\right) \\
\bar{u} = K_p(r - \bar{y}) + \bar{x}_i + C_{\mathrm{aw},2} \bar{x}_{aw,2}
\end{gathered} \tag{34}$$

The steady state of this system is defined by

$$\begin{gathered}
0 = A_p \bar{x}_p + B_p h_\alpha^\beta(\bar{u}; K_p \sigma_n) + B_p d \\
0 = A_{aw,1} \bar{x}_{aw,1} + B_{aw.1}\left(h_\alpha^\beta(\bar{u}; K_p \sigma_n) - \bar{u}\right) \\
0 = A_{aw,2} \bar{x}_{aw,2} + B_{aw.2}\left(h_\alpha^\beta(\bar{u}; K_p \sigma_n) - \bar{u}\right) \\
0 = K_i\left(r - \bar{y} + C_{\mathrm{aw},1} \bar{x}_{aw,1}\right)
\end{gathered} \tag{35}$$

Assuming that the asymptotically stable equilibrium exists

$$\begin{gathered}
0 = K_i\left(r - \bar{y}_{ss} + C_{\mathrm{aw},1} \bar{x}_{aw,1}\right) \\
0 = A_{aw,1} \bar{x}_{aw,1} + B_{aw.1}\left(h_\alpha^\beta(\bar{u}_{ss}; K_p \sigma_n) - \bar{u}_{ss}\right) \\
\bar{y}_{aw,1} = C_{\mathrm{aw},1} \bar{x}_{aw,1}
\end{gathered} \tag{36}$$

According to (36), $\bar{y}_{aw,1}$ is written as below

$$\bar{y}_{aw,1} = -\mathrm{C}_{\mathrm{aw},1} A_{aw,1}^{-1} \mathrm{B}_{\mathrm{aw},1}\left(-\bar{u}_{ss} + h_\alpha^\beta(\bar{u}_{ss}; K_p \sigma_n)\right) = K_{aw,1}(0)\left(\bar{u}_{ss} - h_\alpha^\beta(\bar{u}_{ss}; K_p \sigma_n)\right) \tag{37}$$

Replacing $C_{\mathrm{aw},1} \bar{x}_{aw,1}$ with (37), $\bar{e}_{ss}$ can be defined as below

$$\bar{e}_{ss} = r - \bar{y}_{ss} = K_{aw,1}(0)\left(\bar{u}_{ss} - h_\alpha^\beta(\bar{u}_{ss}; K_p \sigma_n)\right) \tag{38}$$

iv) The system of Figure 4 (d) (PI controlled system with anti-windup introduced in [13]) control input u is defined as below

$$\mathrm{u} = K_p\left(r - \bar{y} - h_\alpha^\beta(\bar{u}; K_p\sigma_n)\left(\frac{s}{K_i + K_p s} - \frac{1}{K_p}\right)\right) \tag{39}$$

The steady state of this system is defined by

$$\bar{u}_{ss} = K_p\left(r - \bar{y}_{ss} - h_\alpha^\beta(\bar{u}_{ss}; K_p\sigma_n)\left(-\frac{1}{K_p}\right)\right) \tag{40}$$

$$\bar{u}_{ss} = K_p\left(\bar{e}_{ss} - h_\alpha^\beta(\bar{u}_{ss}; K_p\sigma_n)\left(-\frac{1}{K_p}\right)\right) \tag{41}$$

Therefore, $\bar{e}_{ss}$ is defined as below

$$\bar{e}_{ss} = r - \bar{y}_{ss} = \frac{1}{K_p}\left(\bar{u}_{ss} - h_\alpha^\beta(\bar{u}_{ss}; K_p\sigma_n)\right) \tag{42}$$

Ⅷ. Appendix Ⅱ

The state space form of Figures 8 (a) is written by

$$\begin{gathered}
\dot{x}_p = A_p x_p + B_p d + B_p sat_\alpha^\beta\left(sat_{\alpha'}^{\beta'}(u)\right) \\
y = C_p x_p \\
\dot{x}_i = K_i(r - y - n) + K_{aw,1}\left(sat_{\alpha'}^{\beta'}(u) - u\right) \\
u = K_p(r - y - n) + x_i
\end{gathered} \tag{43}$$

Applying stochastic averaging theory, (43) is transformed into (44)

$$\begin{gathered}
\dot{\bar{x}}_p = A_p \bar{x}_p + B_p d + B_p h_\alpha^\beta(\bar{u}; K_p\sigma_n) \\
\bar{y} = C_\mathrm{p} \bar{x}_p \\
\dot{\bar{x}}_i = K_i(r - \bar{y}) + K_{aw,1}\left(h_{\alpha'}^{\beta'}(\bar{u}; K_p\sigma_n) - \bar{u}\right) \\
u = K_p(r - \bar{y}) + \bar{x}_i
\end{gathered} \tag{44}$$

According to (44), the block diagram of the system of Figure 8 (a) is replaced with that of Figure 9 (a). Similarly, the state space form of Figures 8 (b) is written by

$$\begin{gathered}
\dot{x}_p = A_p x_p + B_p d + B_p sat_\alpha^\beta\left(sat_{\alpha'}^{\beta'}(u)\right) \\
y = C_p x_p \\
\dot{x}_i = K_i(r - y - n) + K_{aw,1}\left(sat_{\alpha'}^{\beta'}(u) - u\right) \\
u = K_p(r - y - n) + x_i + K_{aw,2}\left(sat_{\alpha'}^{\beta'}(u) - u\right)
\end{gathered} \tag{45}$$

Applying stochastic averaging theory, (45) is transformed into (46)

$$\begin{gathered}
\dot{\bar{x}}_p = A_p \bar{x}_p + B_p d + B_p h_\alpha^\beta(\bar{u}; K_p\sigma_n) \\
\bar{y} = C_\mathrm{p} \bar{x}_p \\
\dot{\bar{x}}_i = K_i(r - \bar{y}) + K_{aw,1}\left(h_{\alpha'}^{\beta'}(\bar{u}; K_p\sigma_n) - \bar{u}\right)
\end{gathered} \tag{46}$$

$$u = K_p(r - \bar{y}) + \bar{x}_i + K_{aw,2}\left(h_{\alpha'}^{\beta'}(\bar{u}; K_p\sigma_n) - \bar{u}\right)$$

According to (46), the block diagram of the system of Figure 8 (b) is replaced with that of Figure 9 (b). The state space form of Figure 8 (c) is written by

$$\begin{aligned} \dot{x}_p &= A_p x_p + B_p d + B_p sat_\alpha^\beta\left(sat_{\alpha'}^{\beta'}(u)\right) \\ y &= C_p x_p \\ \dot{x}_i &= K_i\left(r - y + K_{aw,1}\left(sat_{\alpha'}^{\beta'}(u) - u\right)\right) \\ u &= K_p(r - y) + x_i + K_{aw,2}\left(sat_{\alpha'}^{\beta'}(u) - u\right) \end{aligned} \tag{47}$$

Applying stochastic averaging theory, (47) is transformed into (48). According to (48), the block diagram of the system of Figure 8 (c) is replaced with that of Figure 9 (c).

$$\begin{aligned} \dot{\bar{x}}_p &= A_p \bar{x}_p + B_p d + B_p h_\alpha^\beta(\bar{u}; K_p\sigma_n) \\ \bar{y} &= C_\mathrm{p} \bar{x}_p \\ \dot{\bar{x}}_i &= K_i\left(r - \bar{y} + K_{aw,1}\left(h_{\alpha'}^{\beta'}(\bar{u}; K_p\sigma_n) - \bar{u}\right)\right) \\ u &= K_p(r - \bar{y}) + \bar{x}_i + K_{aw,2}\left(h_{\alpha'}^{\beta'}(\bar{u}; K_p\sigma_n) - \bar{u}\right) \end{aligned} \tag{48}$$

The state space form of Figures 8 (d) is written by

$$\begin{aligned} \dot{x}_p &= A_p x_p + B_p d + B_p sat_\alpha^\beta\left(sat_{\alpha'}^{\beta'}(u)\right) \\ y &= C_p x_p \\ u &= K_p(r - y - n) + y_f \\ \dot{x}_f &= A_f x_f + B_f sat_{\alpha'}^{\beta'}(u) \\ y_f &= C_f x_f \end{aligned} \tag{49}$$

Where, x_f is the state of the function $\frac{s}{K_i + K_p s} - \frac{1}{K_p}$ and y_f is the output of the function. Applying stochastic averaging theory, (49) is transformed into (50)

$$\begin{aligned} \dot{\bar{x}}_p &= A_p \bar{x}_p + B_p d + B_p h_\alpha^\beta(\bar{u}; K_p\sigma_n) \\ \bar{y} &= C_\mathrm{p} \bar{x}_p \\ u &= K_p(r - \bar{y}) + \bar{y}_f \end{aligned} \tag{50}$$

$$\dot{\bar{x}}_f = A_f \bar{x}_f + B_f h_{\alpha'}^{\beta'}(u)$$
$$\bar{y}_f = C_f \bar{x}_f$$

According to (50), the block diagram of the system of Figure 8 (d) is replaced with that of Figure 9 (d).

IX. Appendix Ⅲ

i) The system of Figure 9 (a) (PI controlled system with back-calculation anti-windup)

Let the state space realization of the system of Figure 9 (a) be

$$\begin{aligned} \dot{\bar{x}}_p &= A_p \bar{x}_p + B_p h_{\alpha}^{\beta}(\bar{u}; K_p \sigma_n) + B_p d \\ \dot{\bar{x}}_i &= K_i (r - \bar{y}) + K_{aw,1}\left(h_{\alpha'}^{\beta'}(\bar{u}; K_p \sigma_n) - \bar{u}\right) \\ \bar{y} &= C_{\mathrm{p}} \bar{x}_p \\ u &= K_p (r - \bar{y}) + \bar{x}_i \end{aligned} \tag{51}$$

Where, $\bar{x}_p$, $\bar{x}_i$, $\bar{u}$, d, and $\bar{y}$, and are the state of the plant, the state of the integral controller, the control input, the disturbance of the system and the output of the system of Figure 9 (a) respectively.
The steady state of this system is defined by

$$\begin{aligned} 0 &= A_p \bar{x}_p + B_p h_{\alpha}^{\beta}(\bar{u}; K_p \sigma_n) + B_p d \\ 0 &= K_i (r - \bar{y}) + K_{aw,1}\left(h_{\alpha'}^{\beta'}(\bar{u}; K_p \sigma_n) - \bar{u}\right) \end{aligned} \tag{52}$$

Assuming that the asymptotically stable equilibrium exists

$$0 = K_i (r - \bar{y}_{ss}) + K_{aw,1}\left(h_{\alpha'}^{\beta'}(\bar{u}_{ss}; K_p \sigma_n) - \bar{u}_{ss}\right) \tag{53}$$

Should be satisfied in the steady state, where $\bar{y}_{ss}$ and $\bar{u}_{ss}$ are the steady state values of $\bar{y}$ and $\bar{u}$. Therefore, $\bar{e}_{ss}$ is defined as below

$$\bar{e}_{ss} = r - \bar{y}_{ss} = \frac{K_{aw,1}}{K_i}\left(\bar{u}_{ss} - h_{\alpha'}^{\beta'}(\bar{u}_{ss}; K_p \sigma_n)\right) \tag{54}$$

ii) The system of Figure 9 (b) (PI controlled system with dynamic full authority anti-windup)

Let the state space realization of the system of Figure 9 (b) be

$$\dot{\bar{x}}_p = A_p\bar{x}_p + B_p h_\alpha^\beta(\bar{u}; K_p\sigma_n) + B_p d$$
$$\bar{y} = C_\mathrm{p}\bar{x}_p$$
$$\dot{\bar{x}}_{aw,1} = A_{aw,1}\bar{x}_{aw,1} + B_{aw.1}\left(h_{\alpha'}^{\beta'}(\bar{u}; K_p\sigma_n) - \bar{u}\right)$$
$$\bar{y}_{aw,1} = C_{\mathrm{aw},1}\bar{x}_{aw,1}$$
$$\dot{\bar{x}}_{aw,2} = A_{aw,2}\bar{x}_{aw,2} + B_{aw.2}\left(h_{\alpha'}^{\beta'}(\bar{u}; K_p\sigma_n) - \bar{u}\right)$$
$$\bar{y}_{aw,2} = C_{\mathrm{aw},2}\bar{x}_{aw,2} \tag{55}$$
$$\dot{\bar{x}}_i = K_i(r - \bar{y}) + C_{\mathrm{aw},1}\bar{x}_{aw,1}$$
$$\bar{u} = K_p(r - \bar{y}) + \bar{x}_i + C_{\mathrm{aw},2}\bar{x}_{aw,2}$$

Where, $\bar{x}_{aw,1}$ and $\bar{x}_{aw,2}$ are the state space form of the dynamic anti-windup gain $K_{aw,1}(s)$ and $K_{aw,2}(s)$ respectively. The steady state of this system is defined by

$$0 = A_p\bar{x}_p + B_p h_\alpha^\beta(\bar{u}; K_p\sigma_n) + B_p d$$
$$0 = A_{aw,1}\bar{x}_{aw,1} + B_{aw.1}\left(h_{\alpha'}^{\beta'}(\bar{u}; K_p\sigma_n) - \bar{u}\right)$$
$$0 = A_{aw,2}\bar{x}_{aw,2} + B_{aw.2}\left(h_{\alpha'}^{\beta'}(\bar{u}; K_p\sigma_n) - \bar{u}\right) \tag{56}$$
$$0 = K_i(r - \bar{y}) + C_{\mathrm{aw},1}\bar{x}_{aw,1}$$

Assuming that the asymptotically stable equilibrium exists

$$0 = K_i(r - \bar{y}_{ss}) + C_{\mathrm{aw},1}\bar{x}_{aw,1}$$
$$0 = A_{aw,1}\bar{x}_{aw,1} + B_{aw.1}\left(h_\alpha^\beta(\bar{u}_{ss}; K_p\sigma_n) - \bar{u}_{ss}\right) \tag{57}$$
$$\bar{y}_{aw,1} = C_{\mathrm{aw},1}\bar{x}_{aw,1}$$

According to (57), $\bar{y}_{aw,1}$ is written as below

$$\bar{y}_{aw,1} = -\mathrm{C}_{\mathrm{aw},1}A_{aw,1}^{-1}\mathrm{B}_{\mathrm{aw},1}\left(-\bar{u}_{ss} + h_{\alpha'}^{\beta'}(\bar{u}_{ss}; K_p\sigma_n)\right) = K_{aw,1}(0)\left(-\bar{u}_{ss} + h_{\alpha'}^{\beta'}(\bar{u}_{ss}; K_p\sigma_n)\right) \tag{58}$$

Where, $K_{aw,1}(0)$ is dc gain of the anti-windup gain $K_{aw,1}(s)$. Replacing $C_{\mathrm{aw},1}\bar{x}_{aw,1}$ with (56), $\bar{e}_{ss}$ can be defined as below

$$\bar{e}_{ss} = r - \bar{y}_{ss} = \frac{K_{aw,1}(0)}{K_i}\left(\bar{u}_{ss} - h_{\alpha'}^{\beta'}(\bar{u}_{ss}; K_p\sigma_n)\right) \tag{59}$$

iii) The system of Figure 9 (c) (PI controlled system with dynamic external global anti-windup)

Let the state space realization of the system of Figure 9 (c) be

$$\begin{aligned}
\dot{\bar{x}}_p &= A_p\bar{x}_p + B_p h_\alpha^\beta(\bar{u};K_p\sigma_n) + B_p d\\
\bar{y} &= C_\mathrm{p}\bar{x}_p\\
\dot{\bar{x}}_{aw,1} &= A_{aw,1}\bar{x}_{aw,1} + B_{aw.1}\left(h_{\alpha'}^{\beta'}(\bar{u};K_p\sigma_n) - \bar{u}\right)\\
\bar{y}_{aw,1} &= C_{\mathrm{aw},1}\bar{x}_{aw,1}\\
\dot{\bar{x}}_{aw,2} &= A_{aw,2}\bar{x}_{aw,2} + B_{aw.2}\left(h_{\alpha'}^{\beta'}(\bar{u};K_p\sigma_n) - \bar{u}\right)\\
\bar{y}_{aw,2} &= C_{\mathrm{aw},2}\bar{x}_{aw,2}\\
\dot{\bar{x}}_i &= K_i\left(r - \bar{y} + C_{\mathrm{aw},1}\bar{x}_{aw,1}\right)\\
\bar{u} &= K_p(r-\bar{y}) + \bar{x}_i + C_{\mathrm{aw},2}\bar{x}_{aw,2}
\end{aligned} \tag{60}$$

The steady state of this system is defined by

$$\begin{aligned}
0 &= A_p\bar{x}_p + B_p h_\alpha^\beta(\bar{u};K_p\sigma_n) + B_p d\\
0 &= A_{aw,1}\bar{x}_{aw,1} + B_{aw.1}\left(h_{\alpha'}^{\beta'}(\bar{u};K_p\sigma_n) - \bar{u}\right)\\
0 &= A_{aw,2}\bar{x}_{aw,2} + B_{aw.2}\left(h_{\alpha'}^{\beta'}(\bar{u};K_p\sigma_n) - \bar{u}\right)\\
0 &= K_i\left(r - \bar{y} + C_{\mathrm{aw},1}\bar{x}_{aw,1}\right)
\end{aligned} \tag{61}$$

Assuming that the asymptotically stable equilibrium exists

$$\begin{aligned}
0 &= K_i\left(r - \bar{y}_{ss} + C_{\mathrm{aw},1}\bar{x}_{aw,1}\right)\\
0 &= A_{aw,1}\bar{x}_{aw,1} + B_{aw.1}\left(h_{\alpha'}^{\beta'}(\bar{u}_{ss};K_p\sigma_n) - \bar{u}_{ss}\right)\\
\bar{y}_{aw,1} &= C_{\mathrm{aw},1}\bar{x}_{aw,1}
\end{aligned} \tag{62}$$

According to (62), $\bar{y}_{aw,1}$ is written as below

$$\bar{y}_{aw,1} = -\mathrm{C}_{\mathrm{aw},1}A_{aw,1}^{-1}\mathrm{B}_{\mathrm{aw},1}\left(-\bar{u}_{ss} + h_{\alpha'}^{\beta'}(\bar{u}_{ss};K_p\sigma_n)\right) = K_{aw,1}(0)\left(-\bar{u}_{ss} + h_{\alpha'}^{\beta'}(\bar{u}_{ss};K_p\sigma_n)\right) \tag{63}$$

Replacing $C_{\mathrm{aw},1}\bar{x}_{aw,1}$ with (63), $\bar{e}_{ss}$ can be defined as below

$$\bar{e}_{ss} = K_{aw,1}(0)\left(\bar{u}_{ss} - h_{\alpha'}^{\beta'}(\bar{u}_{ss};K_p\sigma_n)\right) \tag{64}$$

iv) The system of Figure 4 (d) (PI controlled system with anti-windup introduced in [13]) control input u is defined as below

$$u = K_p \left(r - \bar{y} - h_{\alpha'}^{\beta'}(\bar{u}; K_p\sigma_n) \left(\frac{s}{K_i + K_p s} - \frac{1}{K_p} \right) \right) \tag{65}$$

The steady state of this system is defined by

$$\bar{u}_{ss} = K_p \left(r - \bar{y}_{ss} - h_{\alpha'}^{\beta'}(\bar{u}_{ss}; K_p\sigma_n) \left(-\frac{1}{K_p} \right) \right) \tag{66}$$

$$\bar{u}_{ss} = K_p \left(\bar{e}_{ss} - h_{\alpha'}^{\beta'}(\bar{u}_{ss}; K_p\sigma_n) \left(-\frac{1}{K_p} \right) \right) \tag{67}$$

Therefore, $\bar{e}_{ss}$ is defined as below

$$\bar{e}_{ss} = r - \bar{y}_{ss} = \frac{1}{K_p} \left(\bar{u}_{ss} - h_{\alpha'}^{\beta'}(\bar{u}_{ss}; K_p\sigma_n) \right) \tag{68}$$

Ⅹ. Appendix Ⅳ

i) Assume that $K_i \neq 0$, $r \neq 0$ and $d \neq 0$, Let the steady state realization of the system of Figure 4 (b) be

$$
\begin{aligned}
0 = \dot{\bar{x}}_p &= A_p \bar{x}_p + B_p h_\alpha^\beta(\bar{u}; K_p\sigma_n) + B_p d \\
\bar{y} &= C_\mathrm{p}\bar{x}_p \\
0 = \dot{\bar{x}}_{aw,1} &= A_{aw,1}\bar{x}_{aw,1} + B_{aw.1}\left(h_\alpha^\beta(\bar{u}; K_p\sigma_n) - \bar{u}\right) \\
\bar{y}_{aw,1} &= C_\mathrm{aw,1}\bar{x}_{aw,1} \\
0 = \dot{\bar{x}}_{aw,2} &= A_{aw,2}\bar{x}_{aw,2} + B_{aw.2}\left(h_\alpha^\beta(\bar{u}; K_p\sigma_n) - \bar{u}\right) \\
\bar{y}_{aw,2} &= C_\mathrm{aw,2}\bar{x}_{aw,2} \\
0 = \dot{\bar{x}}_i &= K_i(r - \bar{y}) + C_\mathrm{aw,1}\bar{x}_{aw,1} \\
\bar{u} &= K_p(r - \bar{y}) + \bar{x}_i + C_\mathrm{aw,2}\bar{x}_{aw,2}
\end{aligned} \tag{69}
$$

$\bar{y}_{aw,1}$ and $\bar{y}$ are written as below

$$\bar{y}_{aw,1} = -\mathrm{C}_\mathrm{aw,1}A_{aw,1}^{-1}\mathrm{B}_\mathrm{aw,1}\left(-\bar{u} + h_\alpha^\beta(\bar{u}; K_p\sigma_n)\right) = K_{aw,1}(0)\left(\bar{u} - h_\alpha^\beta(\bar{u}; K_p\sigma_n)\right) \tag{70}$$

$$\bar{y} = -\mathrm{C}_\mathrm{aw,1}A_{aw,1}^{-1}\mathrm{B}_\mathrm{aw,1}\left(h_\alpha^\beta(\bar{u}; K_p\sigma_n)\right) \tag{71}$$

By using (70) and (71), $\dot{\bar{x}}_i$ is defined by

$$K_{aw,1}(0)\bar{u} - K_i r = K_i\mathrm{C}_\mathrm{aw,1}A_{aw,1}^{-1}\mathrm{B}_\mathrm{aw,1}\left(h_\alpha^\beta(\bar{u}; K_p\sigma_n)\right) + K_{aw,1}(0)\left(h_\alpha^\beta(\bar{u}; K_p\sigma_n)\right) \tag{72}$$

Similarly, Let the steady state form of $\dot{\bar{x}}_i$ of the system of Figure 9 (b) be

$$K_{aw,1}(0)\bar{u} - K_i r = K_i\mathrm{C}_\mathrm{aw,1}A_{aw,1}^{-1}\mathrm{B}_\mathrm{aw,1}\left(h_\alpha^\beta(\bar{u}; K_p\sigma_n)\right) + K_{aw,1}(0)\left(h_{\alpha'}^{\beta'}(\bar{u}; K_p\sigma_n)\right) \tag{73}$$

By comparing between (72) and (73), the value of $\bar{u}$ that belongs to (72) is greater than that belongs to (73). Therefore, let $\bar{u}$ that belongs to (72) be $\bar{u}_1$ and $\bar{u}$ that belongs to (73) be $\bar{u}_2$. By replacing with $\bar{u}_1$ and $\bar{u}_2$, (72) and (73) are written as below

$$K_{aw,1}(0)\bar{u}_1 - K_i r = K_i \mathrm{C}_{\mathrm{aw},1} A_{aw,1}^{-1} \mathrm{B}_{\mathrm{aw},1} \left(h_\alpha^\beta\big(\bar{u}_1; K_p\sigma_n\big) \right) + K_{aw,1}(0) \left(h_\alpha^\beta\big(\bar{u}_1; K_p\sigma_n\big) \right) \tag{74}$$

$$K_{aw,1}(0)\bar{u}_2 - K_i r = K_i \mathrm{C}_{\mathrm{aw},1} A_{aw,1}^{-1} \mathrm{B}_{\mathrm{aw},1} \left(h_\alpha^\beta\big(\bar{u}_2; K_p\sigma_n\big) \right) + K_{aw,1}(0) \left(h_{\alpha'}^{\beta'}\big(\bar{u}_2; K_p\sigma_n\big) \right) \tag{75}$$

By using (74) and (75) and Assuming that the asymptotically stable equilibrium exists, we can obtain (76)

$$\begin{aligned}
&\mathrm{C}_{\mathrm{aw},1} A_{aw,1}^{-1} \mathrm{B}_{\mathrm{aw},1} \left(h_\alpha^\beta\big(\bar{u}_{1,ss}; K_p\sigma_n\big) - h_\alpha^\beta\big(\bar{u}_{2,ss}; K_p\sigma_n\big) \right) \\
&= \frac{K_{aw,1}(0)}{K_i}\left(\bar{u}_{1,ss} - \bar{u}_{2,ss} - h_\alpha^\beta\big(\bar{u}_{1,ss}; K_p\sigma_n\big) + h_{\alpha'}^{\beta'}\big(\bar{u}_{2,ss}; K_p\sigma_n\big) \right) \\
&= \frac{K_{aw,1}(0)}{K_i}\left(\bar{u}_{1,ss} - h_\alpha^\beta\big(\bar{u}_{1,ss}; K_p\sigma_n\big) \right) - \frac{K_{aw,1}(0)}{K_i}\left(\bar{u}_{2,ss} - h_{\alpha'}^{\beta'}\big(\bar{u}_{2,ss}; K_p\sigma_n\big) \right)
\end{aligned} \tag{76}$$

Where, $\frac{K_{aw,1}(0)}{K_i}\left(\bar{u}_{1,ss} - h_\alpha^\beta\big(\bar{u}_{1,ss}; K_p\sigma_n\big) \right)$ is $\bar{e}_{ss}$ of Figure 4 (b) with dynamic full authority anti-windup and $\frac{K_{aw,1}(0)}{K_i}\left(\bar{u}_{2,ss} - h_{\alpha'}^{\beta'}\big(\bar{u}_{2,ss}; K_p\sigma_n\big) \right)$ is $\bar{e}_{ss}$ of Figure 9 (b) with dynamic full authority anti-windup. According to (72) and (73), $\bar{u}_1$ is greater than $\bar{u}_2$ which means that $h_\alpha^\beta\big(\bar{u}_1; K_p\sigma_n\big)$ is also greater than $h_\alpha^\beta\big(\bar{u}_2; K_p\sigma_n\big)$. Since $\mathrm{C}_{\mathrm{aw},1} A_{aw,1}^{-1} \mathrm{B}_{\mathrm{aw},1}$ is negative value, $\mathrm{C}_{\mathrm{aw},1} A_{aw,1}^{-1} \mathrm{B}_{\mathrm{aw},1} \left(h_\alpha^\beta\big(\bar{u}_{1,ss}; K_p\sigma_n\big) - h_\alpha^\beta\big(\bar{u}_{2,ss}; K_p\sigma_n\big) \right) > 0$ therefore, (76) satisfy

$$\frac{K_{aw,1}(0)}{K_i}\left(\bar{u}_{1,ss} - h_\alpha^\beta\big(\bar{u}_1; K_p\sigma_n\big) \right) - \frac{K_{aw,1}(0)}{K_i}\left(\bar{u}_{2,ss} - h_{\alpha'}^{\beta'}\big(\bar{u}_2; K_p\sigma_n\big) \right) > 0 \tag{77}$$

$$\frac{K_{aw,1}(0)}{K_i}\left(\bar{u}_{1,ss} - h_\alpha^\beta\big(\bar{u}_1; K_p\sigma_n\big) \right) > \frac{K_{aw,1}(0)}{K_i}\left(\bar{u}_{2,ss} - h_{\alpha'}^{\beta'}\big(\bar{u}_2; K_p\sigma_n\big) \right) \tag{78}$$

ii) Assume that the plant of the Figure 4 (b) has a pole at the origin. Since the plant has a pole at the origin, for an equilibrium to exist, the input to the plant should be zero in the steady state, that is,

$$d + h_\alpha^\beta\big(\bar{u}_{1,ss}; K_p\sigma_n\big) = 0 \tag{79}$$

$$d + h_\alpha^\beta\big(\bar{u}_{2,ss}; K_p\sigma_n\big) = 0 \tag{80}$$

where, $h_\alpha^\beta\big(\bar{u}_{1,ss}; K_p\sigma_n\big) = -d$ and $h_\alpha^\beta\big(\bar{u}_{2,ss}; K_p\sigma_n\big) = -d$ which means that $\bar{u}_{1,ss} = \bar{u}_{2,ss}$. Therefore, using (77),

$$\begin{aligned}
&\frac{K_{aw,1}(0)}{K_i}\left(\bar{u}_{1,ss} - h_\alpha^\beta\big(\bar{u}_1; K_p\sigma_n\big) \right) - \frac{K_{aw,1}(0)}{K_i}\left(\bar{u}_{2,ss} - h_{\alpha'}^{\beta'}\big(\bar{u}_2; K_p\sigma_n\big) \right) \\
&= \frac{K_{aw,1}(0)}{K_i}\left(h_{\alpha'}^{\beta'}\big(\bar{u}_{1,ss}; K_p\sigma_n\big) - h_\alpha^\beta\big(\bar{u}_{1,ss}; K_p\sigma_n\big) \right) > 0
\end{aligned} \tag{81}$$

(78) and (81) are completed even when $K_{aw,1}$ is static anti-windup gain because $K_{aw,1}(0)$ is the same with $K_{aw,1}$.

We can figure out that $\left|\bar{u}_{1,ss} - h_{\alpha}^{\beta}(\bar{u}_1; K_p\sigma_n)\right|$ is bigger than $\left|\bar{u}_{2,ss} - h_{\alpha'}^{\beta'}(\bar{u}_2; K_p\sigma_n)\right|$ through Figure 4 (b) and Figure 9 (b), and this fact is applicable to the others. In conclusion, $\left|\bar{u}_{1,ss} - h_{\alpha}^{\beta}(\bar{u}_1; K_p\sigma_n)\right|$ of Figures 4 (a), (b), (c), and (d) are bigger than $\left|\bar{u}_{2,ss} - h_{\alpha'}^{\beta'}(\bar{u}_2; K_p\sigma_n)\right|$ of Figures 9 (a), (b), (c), and (d) respectively.

Ⅺ. Appendix Ⅴ

Let the state space realization of dynamic P gain controller in the system of Figures be

$$\dot{x}_{kp} = A_{kp}x_{kp} + B_{kp}(r - y - n)$$
$$y_{kp} = C_{kp}x_{kp} \tag{82}$$

Where, x_{kp} is the state of dynamic p gain block and y_{kp} is the output of dynamic P gain block. Unlike static P gain controller, a term of $K_p n$ doesn't exist anymore due to dynamic P gain. According to (5) and (8), The function $h_{g_\alpha}^{\beta}(v; K_p\sigma_n)$ is defined as the conditional expected value of $\mathrm{sat}_\alpha^\beta(u)$ in terms of Gaussian distribted noise [10].

$$h_{g_\alpha}^{\beta}(v; K_p\sigma_n) = E_n\left[sat_\alpha^\beta(u)\right] = \int_{-\infty}^{\infty} sat(v - K_p n)\frac{1}{\sqrt{2\pi}\sigma_n}e^{-\frac{n^2}{2\sigma_n^2}}dn \tag{83}$$

Similarly, $h_{u_\alpha}^{\beta}(v; K_p\sigma_n)$ is defined as the conditional expected value of $\mathrm{sat}_\alpha^\beta(u)$ with respect to uniformly distributed noise.

$$h_{u_\alpha}^{\beta}(v; K_p\sigma_n) = E_n\left[sat_\alpha^\beta(u)\right] = \int_{-\sigma_n\sqrt{3}}^{\sigma_n\sqrt{3}} sat(v - K_p n)\frac{1}{2\sigma_n\sqrt{3}}dn \tag{84}$$

Where, u is decomposed into $u = v - K_p n$. v means the portion of u not directly replying on n. As shown in (82), u is decomposed into $u = v$ therefore, Evaluating the integral in (83) and (84) gives (85) and (86).

$$h_{g_\alpha}^{\beta}(v; K_p\sigma_n) = E_n\left[sat_\alpha^\beta(u)\right] = \int_{-\infty}^{\infty} sat(v - K_p n)\frac{1}{\sqrt{2\pi}\sigma_n}e^{-\frac{n^2}{2\sigma_n^2}}dn = sat(v) \tag{85}$$

$$h_{u_\alpha}^{\beta}(v; K_p\sigma_n) = E_n\left[sat_\alpha^\beta(u)\right] = \int_{-\sigma_n\sqrt{3}}^{\sigma_n\sqrt{3}} sat(v - K_p n)\frac{1}{2\sigma_n\sqrt{3}}dn = sat(v) \tag{86}$$

Therefore, $sat(v)$ is not replaced with either $h_{g_\alpha}^{\beta}(v; K_p\sigma_n)$ or $h_{u_\alpha}^{\beta}(v; K_p\sigma_n)$ in spite of applying stochastic averaging theory.

References

[1] K. Johanastrom, and L. Rundqwist. "Integrator windup and how to avoid it." *American Control Conference*, IEEE, 1989.

[2] P.Hippe. *Windup in control: its effects and their prevention*. Springer Science & Business Media, 2006.

[3] Y. Peng, D. Vrancic, and R. Hanus. "Anti-windup, bumpless, and conditioned transfer techniques for PID controllers." *Control Systems, IEEE* 16.4: 48-57, 1996

[4] C, Bohn and D. P. Atherton. "An analysis package comparing PID anti-windup strategies." *Control Systems, IEEE* 15.2: 34-40, 1995.

[5] G. C. Goodwin, S. F. Graebe, and M. E. Salgado, *Control System Design*, Prentice Hall, 2001.

[6] H. A. Fertik and C. W. Ross, “Direct digital control algorithm with antiwindup feature”, *Instrument Society of America*, vol. Preprint, no. 10-1-1CQS-67, 1967.

[7] R. Hanus, “The conditioned control: a new technique for preventing windup nuisances,” in *Proceedings of the International Federation for Information Processing - Automation for Safety in Shipping and Offshore Petroleum Operations*, Trondheim, pp. 221–224, 1980.

[8] A. H. Glattfelder and W. Schaufelberger, “ Stability analysis of single loop control systems with saturation and antireset-windup circuits.” *IEEE Transactions on Automatic Control*, vol. 28, pp. 1074-1081, 1983.

[9] R. Hanus, “A new technique for preventing control windup,” *Journal A*, vol. 21, no. 1, pp. 15–20, 1980.

[10] Y. Eun and E. S. Hamby, “Noise Induced Loss of Tracking in Systems with Saturating Actuators and Antiwindup,” *Journal of Dynamic Systems, Measurement, and Control*, vol. 136, Sep, 2014.

[11] J. Choi, and S. Lee. “Antiwindup strategy for PI-type speed controller.” Industrial Electronics, *IEEE Transactions on Industrial Electronics* vol. 56, no. 6, pp. 2039-2046, 2009.

[12] L. Zaccarian and A. R. Teel, *Modern Anti-windup Synthesis: Control Augmentation for Actuator Saturation*, Princeton University Press, 2011.

[13] G. C. Goodwin, S. F. Graebe, M. E. Salgado; *Control System Design*, Prentice Hall, 2001.

[14] A. V. Skorokhod, “Asymptotic Methods in the Theory of Stochastic Differential Equations,” *American Mathematical Society*, vol. 78, 1989.

[15] Kothare, M. V., et al. "A unified framework for the study of anti-windup designs." *Automatica* 30.12 1869-1883, 1994.

[16] A. Visioli. "Anti-windup strategies." *Practical PID control*: 35-60, 2006.

[17] C. Edwards, and I. Postlethwaite. "Anti-windup and bumpless-transfer schemes." *Automatica* 34.2: 199-

210, 1998.

[18] K. Lehmann, *Gaussian Distributions*, Princeton University, 1997.

[19] K. R. Castleman. *Digital Image Processing*. Prentice Hall, Toronto, 1996

[20] K. Feher. *Telecommunications Measurements: Analysis and Instrumentation*. SciTech Publishing, 1996.

[21] B. Kosko, *Noise,* Viking, 2006.

[22] S. Sastry. *Nonlinear systems: analysis, stability, and control*. Vol. 10. New York: Springer, 1999.

[23] S. Sajjadi-Kia, and F. Jabbari. "Scheduled static anti-windup augmentation synthesis for open-loop stable plants." *American Control Conference (ACC)*, IEEE, 2010.

[24] Yun, K., & Kim, W. J. Microscale position control of an electroactive polymer using an anti-windup scheme. *Smart materials and structures*, *15*(4), 924, 2006.

요 약 문

일반적인 구조의 Anti-windup 기법이 적용된 PI 제어시스템에서의 노이즈에 의한 추종 오차 현상 분석

PI 제어기는 다양한 산업 분야에서 폭넓게 활용되고 있고 추종 오차를 제거하는데 중요한 역할을 한다. 포화 동작기를 가진 PI 제어시스템에서는 시스템의 성능을 저하시키는 Windup 이란 현상이 발생하는데 이를 막기 위해 Anti-windup 이라고 불리는 기법이 적용된다. Anti-windup 기법이 적용된 PI 제어시스템에서 최근에 가우시안 분포 특성을 가진 측정노이즈로 인한 추종 오차가 발생하는 것을 확인하였는데 그 원인은 측정 노이즈가 지속적으로 Anti-windup 동작을 일으키기 때문이다. 이런 현상을 Noise-Induced Tracking Error 즉, NITE 라고 명명하였다 [10]. 이 현상이 발견된 시스템에 적용된 Anti-windup 기법은 back-calculation 이라고 불리는 기법으로서 일반적인 Anti-windup 구조 중에 하나이다.

본 연구에서는 NITE 현상이 back-calculation 기법이 적용된 시스템에서 나타나는 것뿐만 아니라, 일반적인 모든 Anti-windup 구조에서도 나타날 수 있음을 보여주었다. 우리는 일반적인 구조의 Anti-windup 기법이 적용된 PI 제어시스템에서 발생하는 NITE 현상을 분석하기 위해, 확률적 평균 이론을 적용하여 NITE 를 시스템의 매개변수와 노이즈의 특성에 대한 식으로 정량화하였다. 또한, NITE 현상은 노이즈의 분포 특성에 관계없이 나타나는데 이를 가우시안 분포 특성을 가진 노이즈인 경우와 균등 분포 특성을 가진 노이즈인 경우를 서로 비교를 수행하였다.

NITE 를 효과적으로 피할 수 있는 두 가지 방법에 대해서 언급을 하였다. 실제 포화 동작기의 입력신호로서 가상의 포화기를 적용하는 방법이다. 포화 작동기와 가상의 포화기가 포함된 이런 시스템은 비선형특성을 가지므로 리아푸노프 이론을 적용하여 선형 행렬 부등식의 형태로 나타내었고 이를 활용하여 내부 안정도를 판별할 수 있다. NITE 를 줄이는 또 한가지 방법은 해석 PI 제어기의 비례적분기의 이득을 dynamic 의 형태로 바꾸는 것이다. 언급된 두 가지 방법을 통해 실제로 NITE 가 줄어드는 것을 보여주었다.

핵심어: Noise induced tracking error, General anti-windup strategies, 포화 동작기, PI 제어, 측정 노이즈

Acknowledgement

석사과정을 끝내는데 도움을 주시고 저를 잘 이끌어 주시고 제어 분야에 큰 흥미를 느끼게 만들어 주신 은용순 교수님께 먼저 감사의 말씀을 드립니다. 학교에서 어려움이 있었을 때, 교수님의 배려로 제가 석사과정을 잘 끝마칠 수 있었고 부족한 저에게 끊임없이 조언을 해주시며 연구자로서의 길로 이끌어 주시고 진심으로 감사 드립니다. 더불어 좋은 사람들을 만나게 돼서 매우 기쁘게 생각합니다.

지도교수님뿐만 아니라 제 석사 논문을 지도해주신 박경준 교수님과 로봇공학의 김종현 교수님께도 감사의 말씀을 드립니다. 박경준 교수님과 김종현 교수님이 조언해주시고 지적해 주신 연구방향은 앞으로의 연구하는데 있어서 큰 밑거름이 될 것이라고 생각합니다.
뿐만 아니라, 제가 지금 이 자리에 있을 수 있도록 도와주신 에너지공학과의 홍승태 교수님을 비롯 여러 교수님께 감사 드리고, 권욱현 석좌교수님, 손상혁 대학원장님, 장재은 교수님, 최지웅 교수님, 최지환 교수님, 김민수 교수님, 황제윤 교수님, 제민규 교수님께도 감사의 말씀을 드립니다.

그리고 저를 항상 믿어주시고 묵묵히 응원해주시는 사랑하는 부모님과 가장 아끼는 내 동생 주명이 주훈이, 그리고 친척분들께 감사의 말을 드립니다. 석사과정 동안 같이 연구실 생활을 한 성민이형, 부연이형, 희균이형, 유창이형, 기훈이형, 동민이형, 규진이형, 재근이 모두에게 감사의 말을 전합니다. 또한, 저를 오랫동안 보면서 같이 지낸 소중한 친구들 병웅이, 민수, 광호, 효진이, 호진이 그리고 현재, 치승이, 민석이 모두에게 감사의 말을 전합니다.

여기에 다 언급하지는 못했지만, 저를 오랫동안 보면서 같이 지낸 여러 주변 분들께 모두 감사의 말씀을 드립니다. 앞으로 연구하는데 있어서 더 노력하고 계속해서 발전하는 제가 되도록 하겠습니다.